NASA CR-111889-A

DEMONSTRATION OF A STERILIZABLE SOLID ROCKET MOTOR SYSTEM

CONTRACT NAS1-10086

DECEMBER 1971

aerojet solid propulsion company

P. O. BOX 13400 SACRAMENTO, CALIFORNIA 95813 • A DIVISION OF AEROJET-GENERAL

DEMONSTRATION OF A STERILIZABLE SOLID ROCKET MOTOR SYSTEM

Contract NAS1-10086

ADDENDUM TO THE FINAL REPORT

December 1971

Prepared by:

D. O. DePree
W. L. Lambert

aerojet solid propulsion company

A GENERAL TIRE & RUBBER COMPANY

TABLE OF CONTENTS

LIST OF FIGURES

LIST OF FIGURES (cont.)

INTRODUCTION

This report is an addendum to NASA CR-111889, the final report for the basic effort under Contract NAS1-10086, Demonstration of a Sterilizable Solid Rocket Motor System. The scope of effort was expanded by Contract Change Number 3 for the purpose of performing certain tasks leading to the application of the developed technology to a flight-weight motor. The sterilizable propellant was to be reformulated to a total solids loading of 84% and to a lower modulus of elasticity of approximately 1170 N/cm^2 (1700 psi) in order to improve mechanical properties. A detailed stress analysis was to be performed on two types of grain designs for the SVM-3 spherical motor case, (1) a conventionally case-bonded configuration and (2) a partially (or intermittently) bonded configuration having a thicker propellant web.

The technical emphasis was placed on characterization of a scaled-up batch of the improved propellant formulation and determination of the effects of dry heat sterilization on propellant integrity and structural response. The grain stress analysis was directed toward tailoring a fully-bonded grain to the calculated propellant allowable stresses and investigating various bond-release concepts to relieve stresses incurred in thermal shrinkage following sterilization.

SUMMARY

This report describes the work performed by the Aerojet Solid Propulsion Company in fulfillment of the requirements of Modification Number 3 to NASA Contract NAS1-10086, and, as such, is an addendum to Report CR-111889, the final report for the initial effort under this contract. The principal activities in this phase were the characterization of a modified sterilizable solid propellant formulation, designated ANB-3289-3; determination of the effects of dry heat sterilization on the propellant integrity and structural response; and analysis of the structural behavior of sterilizable propellant grains in an SVM-3 spherical motor case.

The ANB-3289-2 sterilizable propellant formulation demonstrated in the initial phase of this program was modified by reducing the total solids content from 85 to 84 wt% and by reducing the initial modulus (E_o) from 1379 N/cm^2 (2000 psi) to 1172 N/cm^2 (1700 psi) in order to improve the mechanical properties. The modified formulation (ANB-3289-3) was scaled up by mixing a 75 Kg (165 lb) batch. The mechanical and physical properties were characterized in an extensive series of tests. In general, the properties were only slightly changed, although under some conditions the strain capability increased and bond strength decreased to a greater extent than would be expected from the lower modulus.

The effect of exposure of the propellant to six 53-hour sterilization cycles at 135°C (275°F) was evaluated. Mechanical properties and solid strand burning rates were unchanged by sterilization, confirming the basic chemical stability of the system.

Tests were conducted to determine the effective stress-free temperature resulting from sterilization. An unexpectedly high rate of stress relaxation, or plastic flow, was indicated under the compressive stress conditions encountered with a cast-in-case grain. Test results indicated a nearly complete shift from the 62°C (135°F) cure temperature to the 135°C (275°F) sterilization temperature. It is also apparent that the shift is highly sensitive to the load-path incurred during the sterilization cycle.

Grain designs for the SVM-3 motor case envelope were analyzed on the basis of the ANB-3289-3 propellant and ANB-3289-3/SD-886/4030 bond characterization data. Bond tensile stress was found to be more critical than either bond shear-stress or inner bore hoop strain. In the case of a fully-bonded grain, the web had to be reduced to about 5.1 cm (2.0 in.) for the 45.0 cm (17.7 in.) dia motor to obtain positive margins for the thermal shrinkage condition from the apparent stress-free temperature to 21°C (70°F). Various bond release patterns were relatively ineffective for reducing the maximum bond tensile stress of thicker web grains, although bore strains could be sharply reduced.

It is concluded that, although the propellant-liner-insulation system can successfully withstand the required heat sterilization conditions without degradation, the relatively low propellant strength and the large shift in stress-free temperature combine to limit the application of this propellant formulation in a case-bonded grain to relatively low volumetric loading configurations. Pending improvements in the propellant characteristics, a stress-relieving grain retention system will be necessary for achievement of high volumetric loading.

It is recommended that further effort be applied toward improving the propellant binder system by upgrading the backbone polymer and by re-evaluating the function of the bonding agent. It is also recommended that more sophisticated stress-relieving grain retention systems be evaluated, and that load-path relationships be explored for the means to reduce the apparent stress-free temperature shift during sterilization.

TECHNICAL DISCUSSION

A. PROPELLANT REFORMULATION

ANB-3289-2 propellant was reformulated from a total solids level of 85 wt% to 84 wt% to provide a propellant having potentially greater strain capability. The net change of one percent was effected by reducing the oxidizer content from 67 wt% to 66 wt%. The solids composition of 66 wt% stabilized ammonium perchlorate and 18 wt% aluminum provides optimum specific impulse at the 84 wt% level.

ANB-3289-2 formulation was additionally modified by reducing the trimethylolpropane (TMP) crosslinker concentration from 43 equivalents to 41 equivalents. This modification was made to lower the propellant modulus from 1379 N/cm^2 (2000 psi) to approximately 1172 N/cm^2 (1700 psi) based on the 85 wt% solids formulation, thus improving the strain capability. The lower modulus level had previously been demonstrated to resist porosity formation during heat sterilization in propellant blocks with cross-sections of the order of 7.6 cm (3 inches).

The effect of the reduction in total solids from 85 to 84% and a modification in the crosslinker concentration on mechanical properties at 25°C (77°F) and solid strand burning rate was determined in 0.45 kg (1 lb) propellant batches.

Three 0.45 kg (1 lb) propellant batches of the modified formulation designated ANB-3289-3, were prepared with purified Telagen-S polymer left over from the initial study. The mechanical properties of the cured propellant at 25°C (77°F) are as follows:

σ_m, N/cm^2 (psi)	ε_m, %	ε_b, %	E_o, N/cm^2 (psi)
103 (149)	19	30	955 (1385)

Three oxidizer grind ratios (80/20, 70/30 and 60/40) Ung/HSMP were prepared and the effect of oxidizer grind ratio on solid strand burning rate determined over a pressure range of 217 to 561 N/cm^2 (300 to 800 psig). A plot showing the effect of oxidizer blend ratio on the solid strand burning rate at 355 N/cm^2 (500 psig) is shown in Figure 1. These data demonstrated the ability to adjust the burning rate of ANB-3289-3 propellant over a limited range to meet motor design requirements.

B. SCALE-UP OF ANB-3289-3 PROPELLANT

A 75 kg (165-lb) batch of the modified propellant formulation ANB-3289-3 was prepared in the 0.11 m^3 (30 gal) vertical mixer to evaluate scale-up effects. The same mixer will be used to prepare propellant batches for casting motors in the follow-on motor demonstration program.

Raw materials for the preparation of the scale-up batch and subsequent motor batches were not available as off the shelf items. It was necessary to process Telagen-S prepolymer to remove iron and silicon contamination.

A total of 34.5 kg (76 lbs) of purified Telagen-S, secondary hydroxyl-terminated saturated polybutadiene, (lot #316AM-5 blend) was recovered from the purification and vacuum stripping of approximately 36.3 kg (80 lbs) of starting material.

Analysis of the purified polymer showed the contaminants had been sufficiently removed. The iron content was reduced to less than two parts per million and the silicon to four parts per million. The equivalent weight was reduced from 1120 to 1036. The product polymer achieved a brown coloration during processing. This coloration was traced to the extraction by the toluene solvent of a hindered phenol antioxidant from the rubber O-rings in the Alsop filter used to remove the carbon black absorbent. Identification of the t-butyl substituted antioxidant was made by means of NMR examination of the polymer products, untreated polymer and a toluene extract (colored) of the O-rings. Color is imparted by the

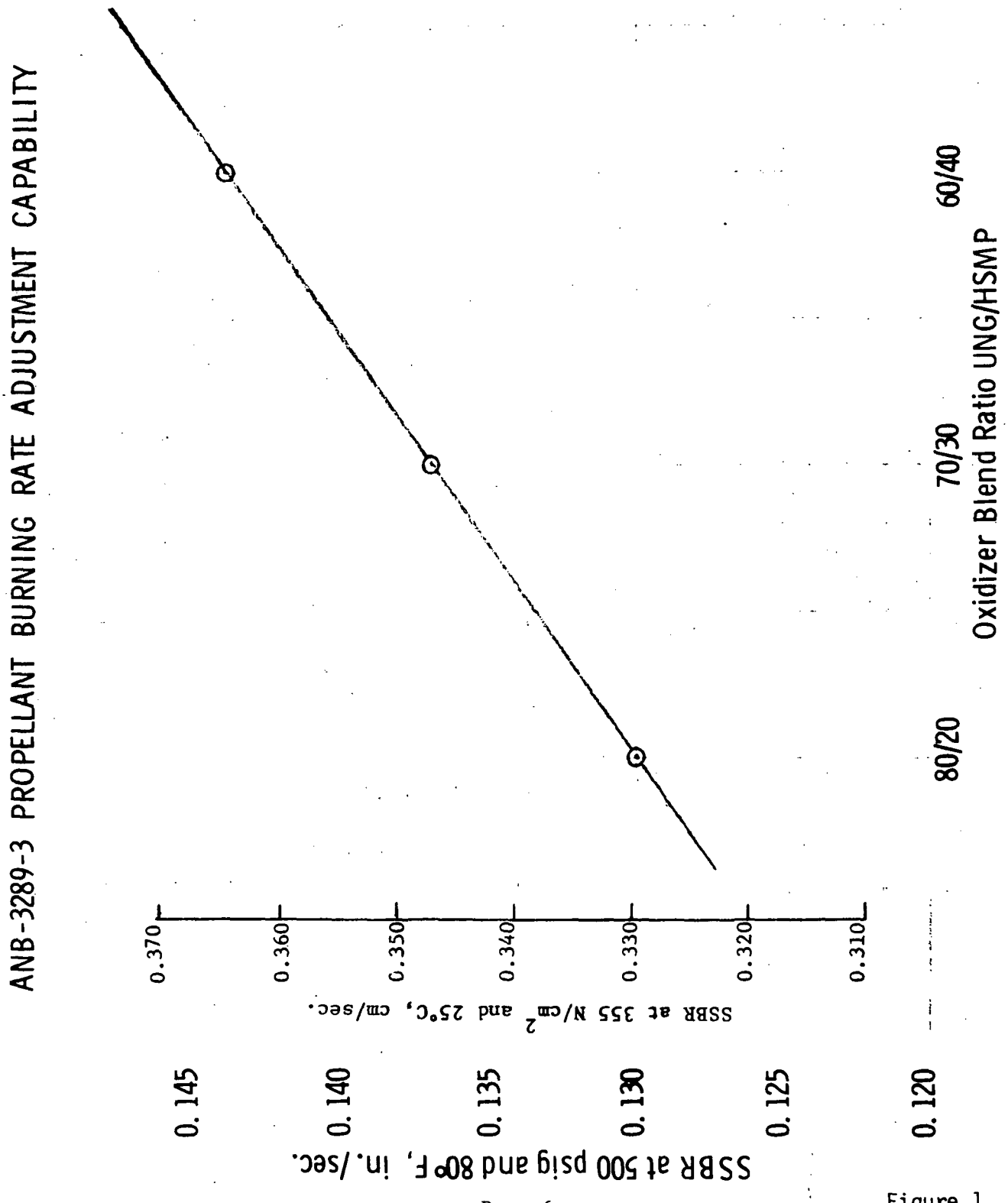
ANB-3289-3 PROPELLANT BURNING RATE ADJUSTMENT CAPABILITY
SSBR at 500 psig and 80°F, in./sec.
0.145
0.140
0.135
0.130
0.125
0.120
SSBR at 355 N/cm² and 25°C, cm/sec.
0.370
0.360
0.350
0.340
0.330
0.320
0.310
80/20
70/30
60/40
Oxidizer Blend Ratio UNG/HSMP

Figure 1

quinoid structure (oxidized) of the antioxidant. The presence of a minute concentration of a non-volatile antioxidant should have no effect on the stability of the polymer during sterilization.

The oxidizer grind ratio used in the scale-up batch was 80 Unground/20 HSMP. DTA examination of the freshly ground HSMP, Figure 2, showed the oxidizer to be essentially unaffected by additional storage as shown by the small impurity peak occurring at 350°C. The oxidizer remained very dry as indicated by the following analytical results:

	Moisture, wt%	
	Surface	Total
Blend	-	0.012
Unground	0.007	-
HSMP	0.009	-

Processing characteristics of the scaled-up propellant were found to be excellent. Observation of the propellant flow behavior during the casting of numerous samples confirmed the viscosity tests which indicated propellant potlife in excess of eight hours. Figure 3 shows the propellant viscosity buildup at 57°C (135°F). A plot of the same propellant viscosity data as a function of shear stress (Figure 4) a good measure of propellant flow behavior, indicates little if any, pseudoplasticity. The lack of pseudoplasticity is a very desirable propellant characteristic. Propellants of this type reliably result in void free motors.

The propellant was cured at 135°F and exhibited normal cure behavior. To assess how scaling effects this propellant, a 0.45 kg (1 lb) batch was prepared using the identical raw materials as used in the 75 kg (165 lb) batch. A comparison of the mechanical properties from the two batches is shown below and indicates excellent agreement was obtained between the laboratory-scale and full-scale mixes.

Batch Size, kg (lbs)	Mechanical Properties at 25°C (77°F)			
	σ_m, (N/cm^2) (psi)	ε_m, %	ε_b, %	E_o (N/cm^2 (psi)
0.45 (1)	112 (163)	17	21	1181 (1713)
75 (165)	106 (154)	14	20	1140 (1654)

DIFFERENTIAL THERMOGRAM OF HSMP OXIDIZER FROM STABILIZED AMMONIUM PERCHLORATE

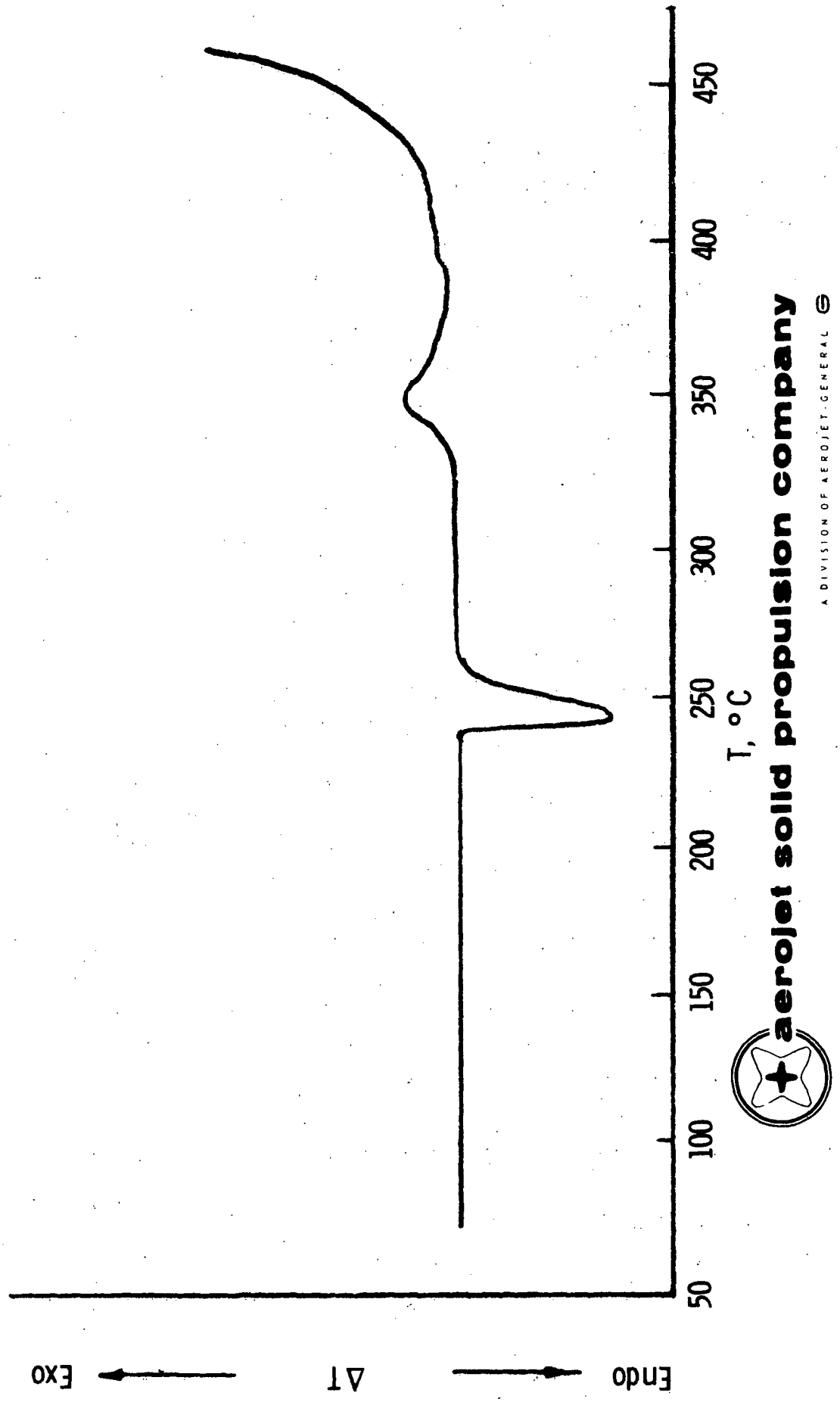

Figure 2

VISCOSITY BUILDUP OF ANB-3289-3 PROPELLANT PREPARED IN 0.11 M^3 (30 Gal) MIXER
(Batch 71-63)

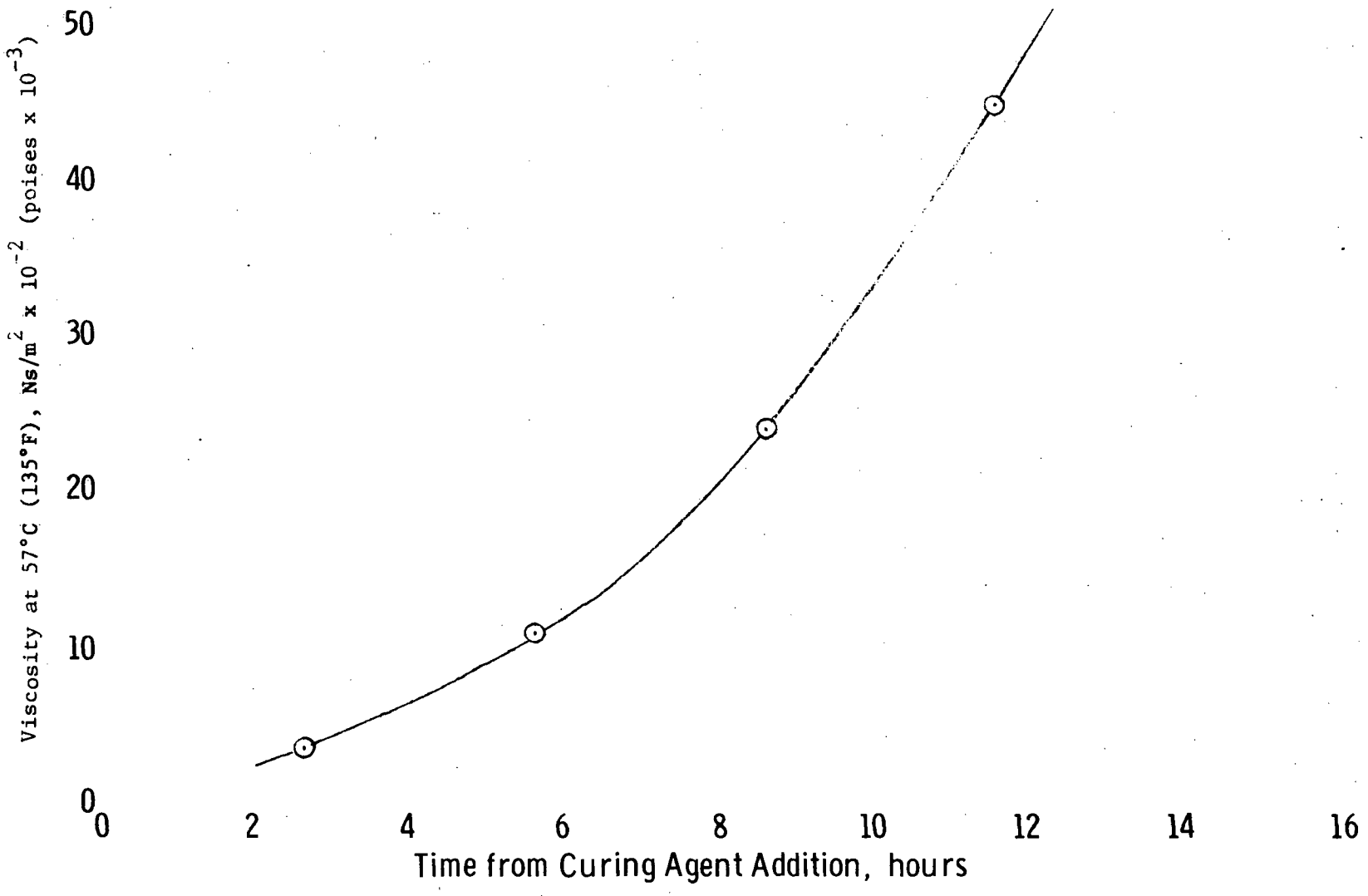

Figure 3

PROPELLANT VISCOSITY AS A FUNCTION OF SHEAR STRESS AND TIME FROM CURING AGENT ADDITION

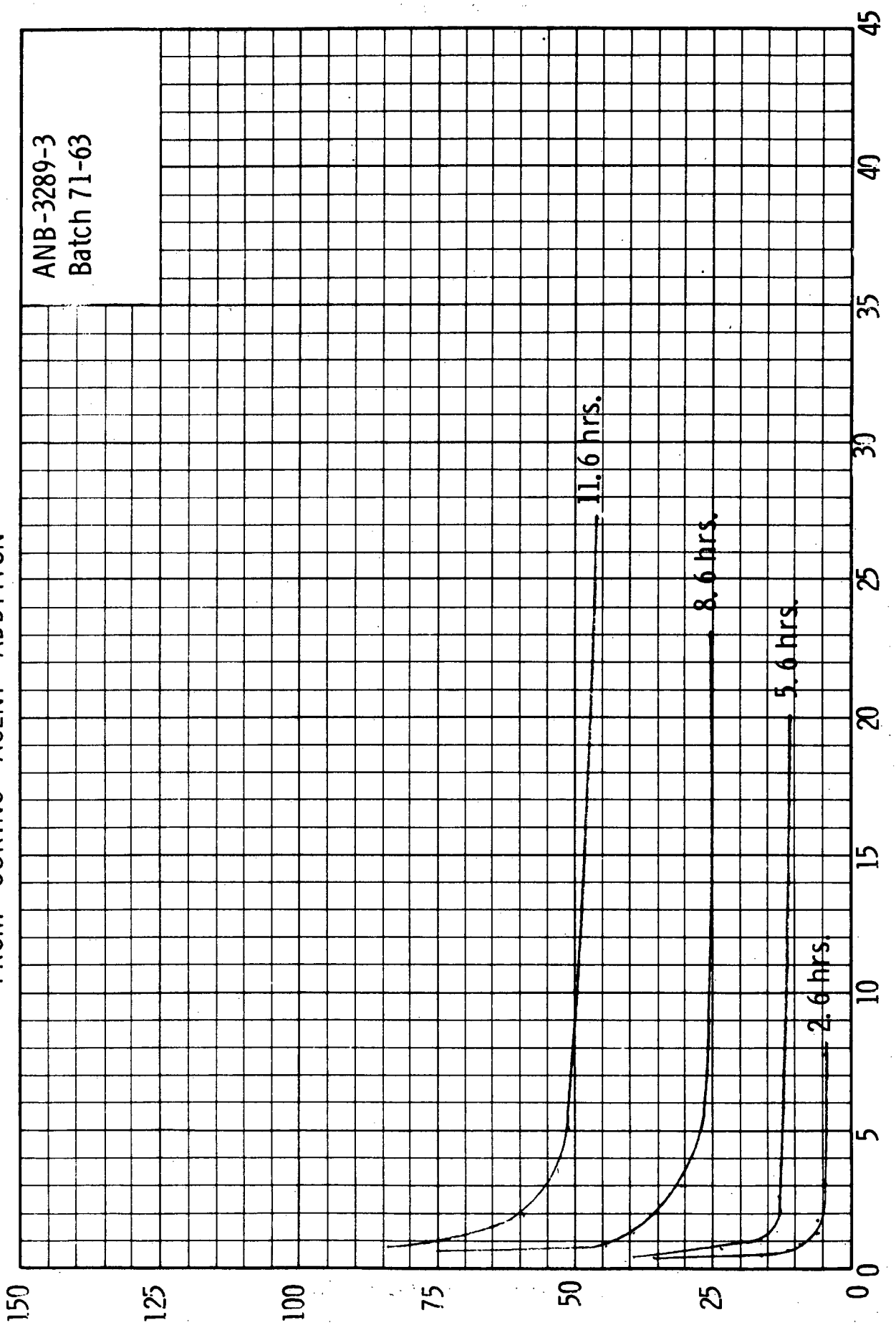

Figure 4

The increase in propellant modulus of these batches compared to the initial 0.45 kg (1 lb) batch data of 955 N/cm^2 (1385 psi) reflect the change in polymer lot and relatively less efficient stripping of the polymer on the pilot-scale wipe film still.

Propellant from the 75 kg (165-lb) batch (71-63) was subjected to a complete mechanical and bond allowables characterization program. This study indicated only a slight improvement in strain capability was realized from the lower solids loaded propellant. Data showing the effect of strain rate and temperature on the uniaxial tensile properties of the propellant are presented in Figure 5. The effect of reduced strain rate (εa_T) on the strain characteristics of ANB-3289-3 propellant is compared with ANB-3289-2 propellant in Figure 6. As can be seen from this plot there is an overall small improvement in the strain capability of ANB-3289-3 reflecting the lowered solids content and the resultant lower modulus. A comparison of the effect of tensile stress on time to failure for the two propellant modifications is presented in Figure 7. Here the reduced solids loading resulted in a slightly lowered tensile strength. The effect of reduced strain rate on propellant modulus is presented in Figure 8.

The effect of temperature and strain rate at 217 N/cm^2 (300 psig) pressure on the uniaxial tensile properties of ANB-3289-3 propellant were determined at 4 and 25°C (40 and 77°F). These data are shown in Figure 9.

Plots of the strain rate data comparing ANB-3289-3 with ANB-3289-2 propellant, including measurements made at both ambient and 217 N/cm^2 (300 psig) pressure, are shown in Figure 10.

The relaxation modulus as a function of temperature for the two propellant modifications are shown in Figure 11. Master time shifted plots are shown in Figure 12 and a plot showing allowable strains at rates typical of motor ignition is shown in Figure 13. A comparison of the master relaxation curves for ANB-3289-3 and ANB-3289-2 propellants is presented in Figure 14. The master curve for ANB-3289-3 does not show the discontinuity previously found in the data obtained with ANB-3289-2 propellant. This discontinuity occurring at 93°C (200°F) has

EFFECT OF TEST TEMPERATURE AND STRAIN RATE ON UNIAXIAL TENSILE PROPERTIES[1] OF ANB-3289-3 PROPELLANT: BATCH 71-63 (HEAT STERILIZABLE PROPELLANT)

Test Temp. °C (°F)	Strain Rate $min.^{-1}$	σ_m N/cm^2 (psi)	ε_m %	ε_b %	E_o N/cm^2 (psi)	Shore "A"
135 (275)	0.074	29 (42)	5.6	7.0	666 (966)	76
	0.74	37 (54)	6.0	6.6	761 (1104)	76
121 (250)	0.074	33 (48)	5.8	7.0	740 (1074)	75
	0.74	41 (59)	6.2	8.3	896 (1300)	76
93 (200)	0.074	43 (62)	6.4	6.6	813 (1180)	76
	0.74	54 (78)	8.0	10.0	896 (1300)	76
65 (150)	0.074	50 (72)	8.2	8.8	803 (1165)	75
	0.74	65 (95)	9.7	11.1	918 (1332)	76
43 (110)	0.074	63 (91)	9.8	11.0	881 (1278)	76
	0.74	81 (118)	12.1	14.0	1025 (1486)	74
	7.4	98 (142)	14.0	22.2	1449 (2100)	76
25 (77)	0.074	79 (115)	13.0	15.6	927 (1344)	76
	0.74	101 (146)	15.6	22.6	1156 (1676)	76
	7.4	128 (186)	16.9	36.8	1777 (2578)	76
14 (57)	7.4	154 (224)	16.7	37.2	2141 (3106)	76
4 (40)	0.074	143 (207)	14.6	20.6	2503 (2630)	76
	0.74	172 (250)	16.9	22.0	2395 (3473)	77
-18 (0)	0.74	534 (775)	10.5	13.8	10869 (15764)	78

(1) Mean value based on two specimens tested at each condition.

Figure 5

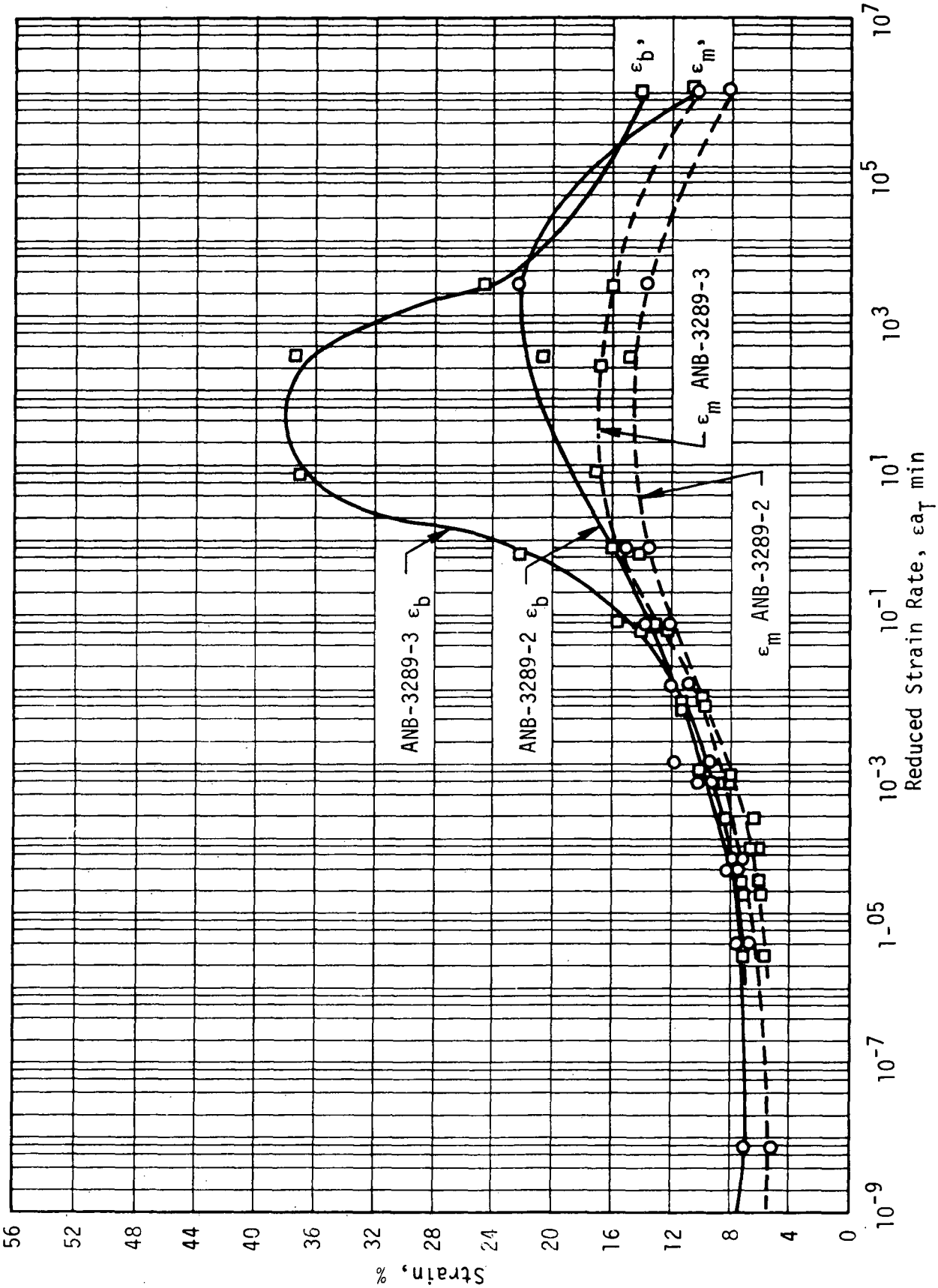

Effect of Reduced Strain Rate on the Strain Characteristics of ANB-3289 Propellant

Figure 6

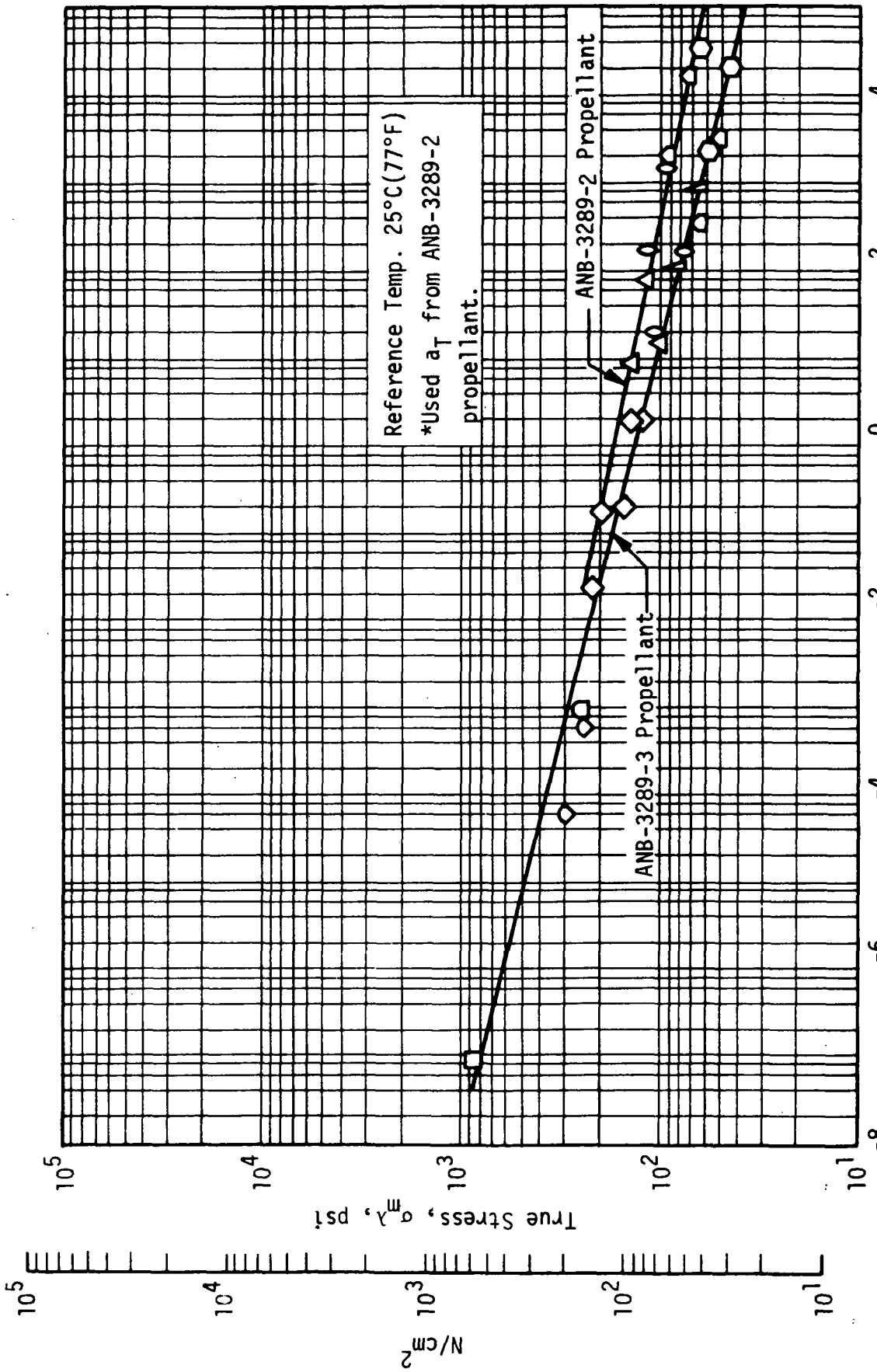

Effect of Stress on Reduced Time to Maximum Stress for ANB-3289 Propellants

Figure 7

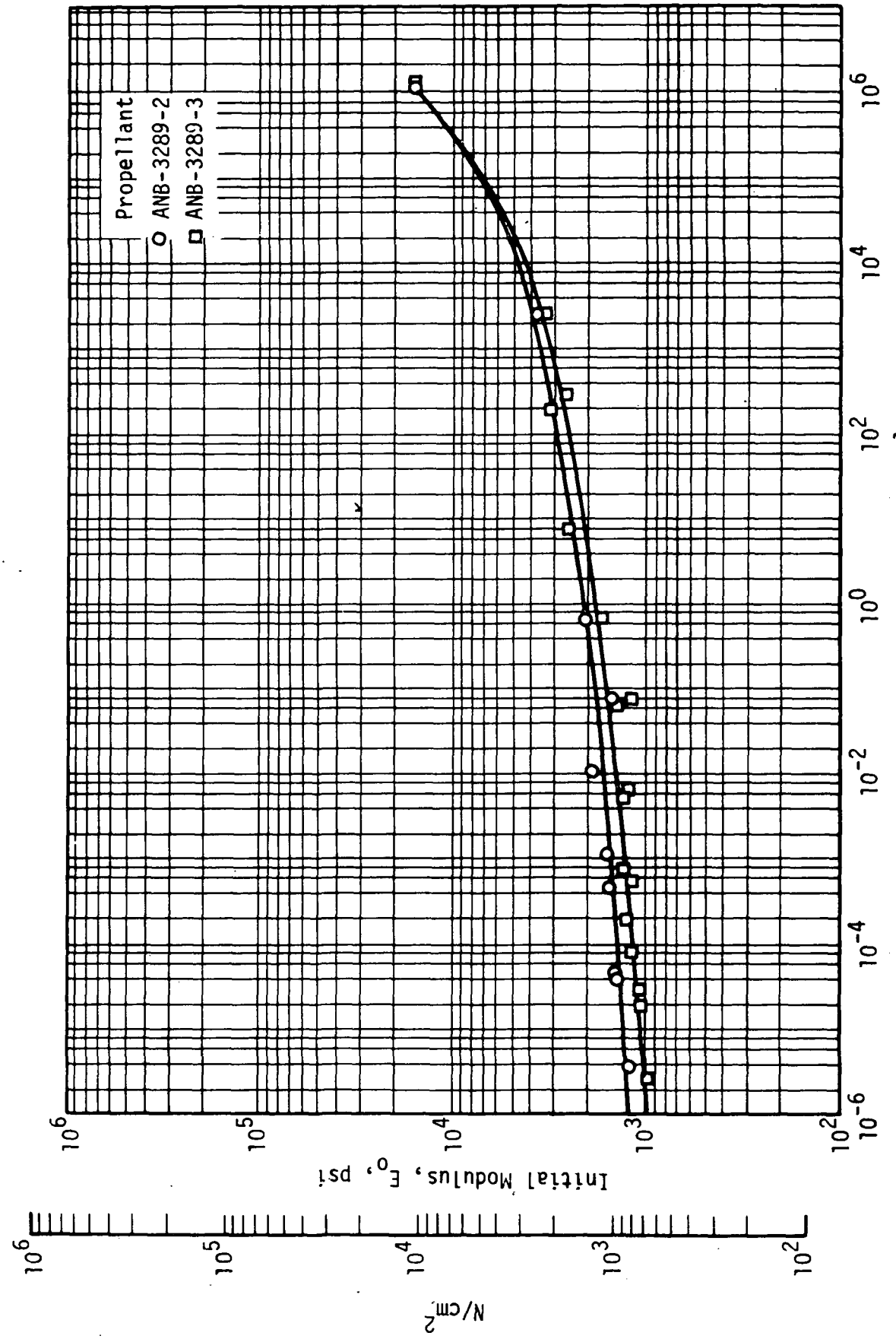

Effect of Reduced Strain Rate on Initial Modulus for ANB-3289-2 and ANB-3289-3 Propellants

Figure 8

EFFECT OF TEST TEMPERATURE AND STRAIN RATE ON UNIAXIAL TENSILE PROPERTIES[1]
ANB-3289-3 PROPELLANT: BATCH 71-73

Test Temp. °C (°F)	Strain Rate, $min.^{-1}$	σ_m N/cm^2 9psi)	ϵ_m o/o	ϵ_b o/o	E_o N/cm^2 (psi)
25 (77)	10	224 (325)	26.8	32.0	1641 (2380)
	100	285 (414)	27.4	39.0	2461 (3570)
	1000	416 (603)	21.2	36.4	4064 (5895)
4 (40)	10	319 (463)	21.0	28.8	3840 (5570)
	100	429 (622)	18.0	30.1	5998 (8700)
	1000	634 (919)	13.0	20.8	12031 (17450)

(1) Mean value from two specimens tested at each condition.

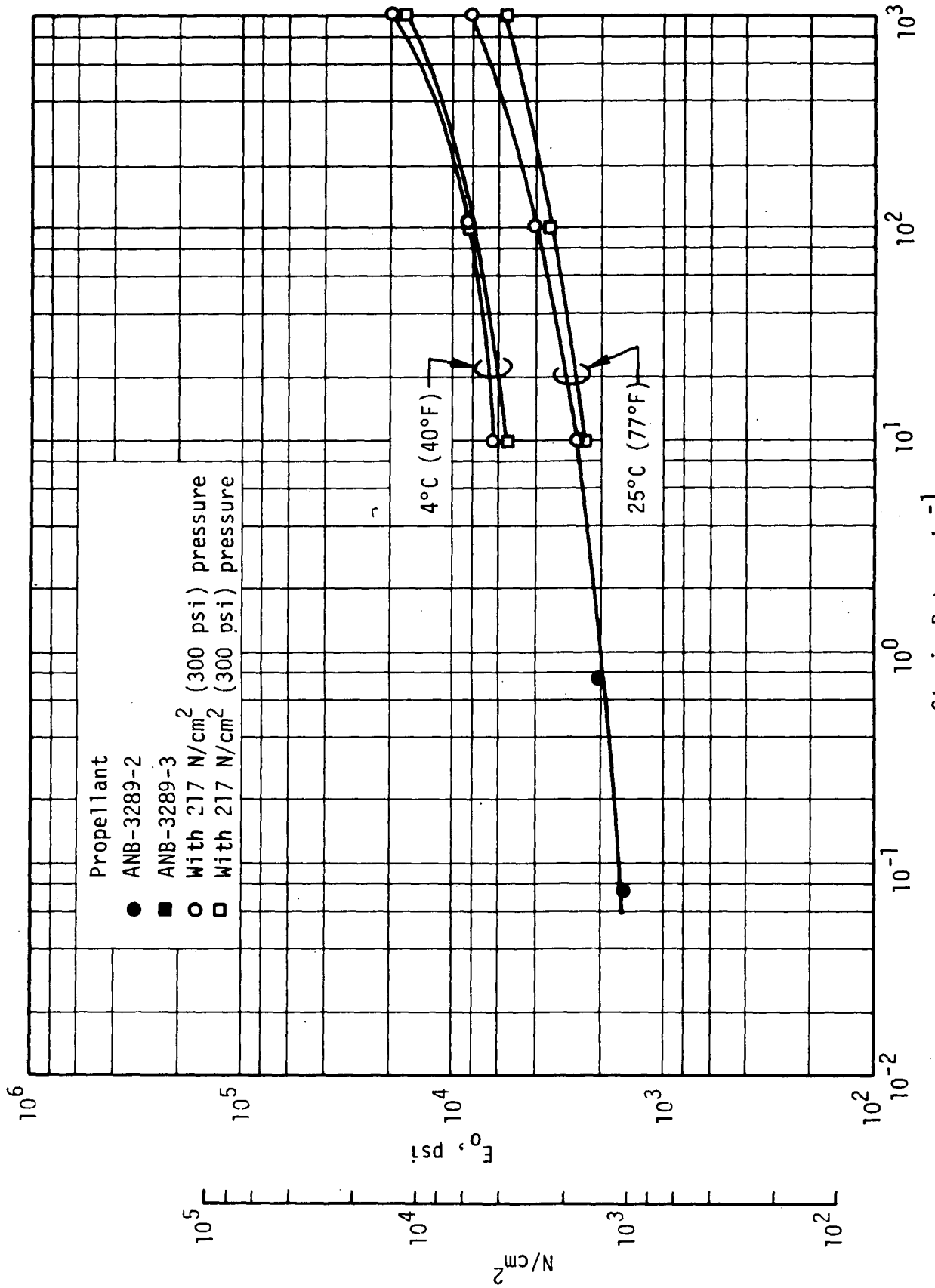

Effect of Temperature, Strain Rate, and Pressure on Initial Tangent Modulus: ANB-3289 Propellant Modifications

Figure 10

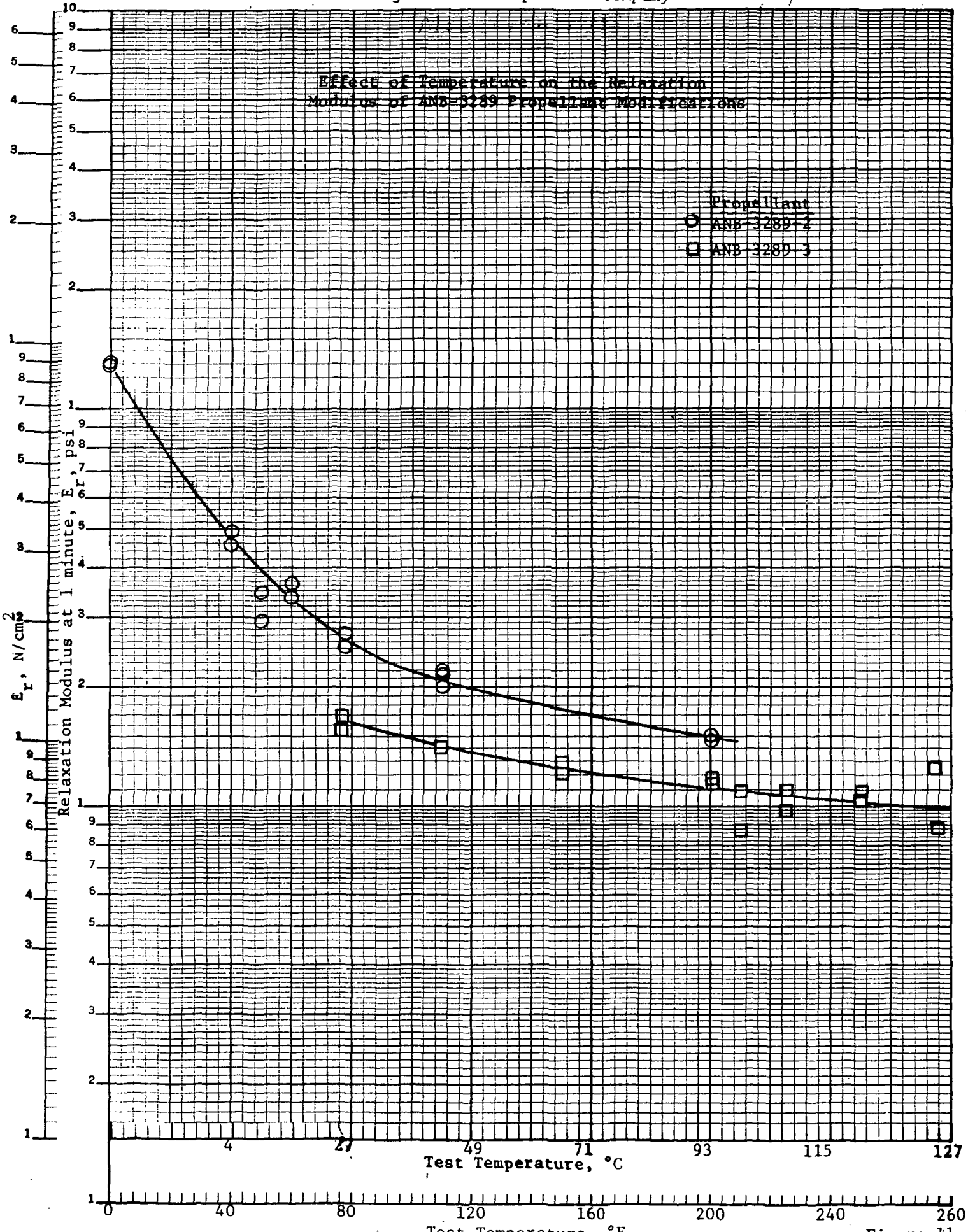
Effect of Temperature on the Relaxation Modulus of ANB-3289 Propellant Modifications
Propellant
ANB-3289-2
ANB-3289-3
Relaxation Modulus at 1 minute, E_r, psi
E_r, N/cm^2
Test Temperature, °C
Test Temperature, °F
4
21
49
71
93
115
127
0
40
80
120
160
200
240
260

Figure 11.

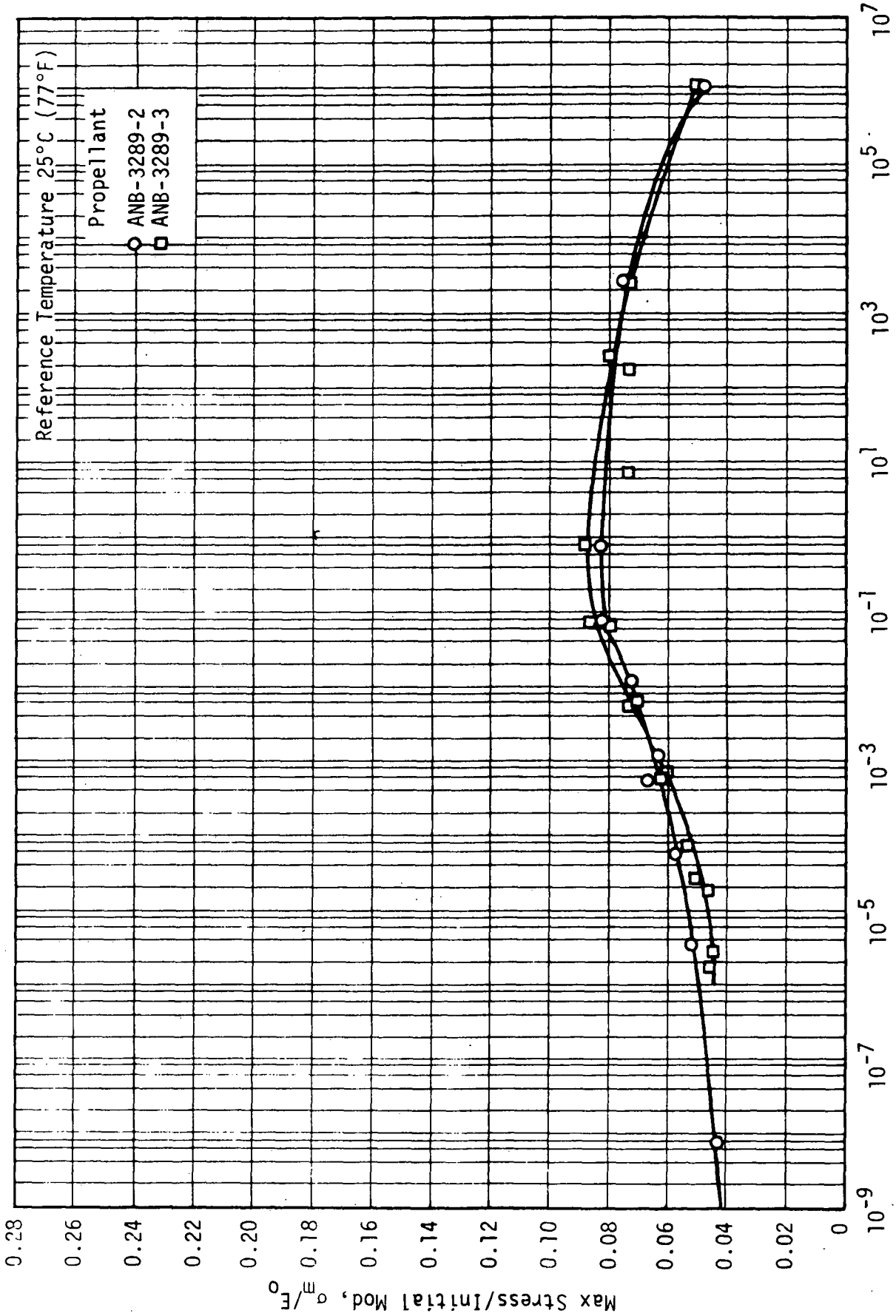

Effect of Reduced Strain Rate on Maximum Nominal Stress to Initial Modulus for ANB-3289 Propellant Modifications

Figure 12

ALLOWABLE STRAIN FOR FIRING FOR ANB-3289 PROPELLANTS

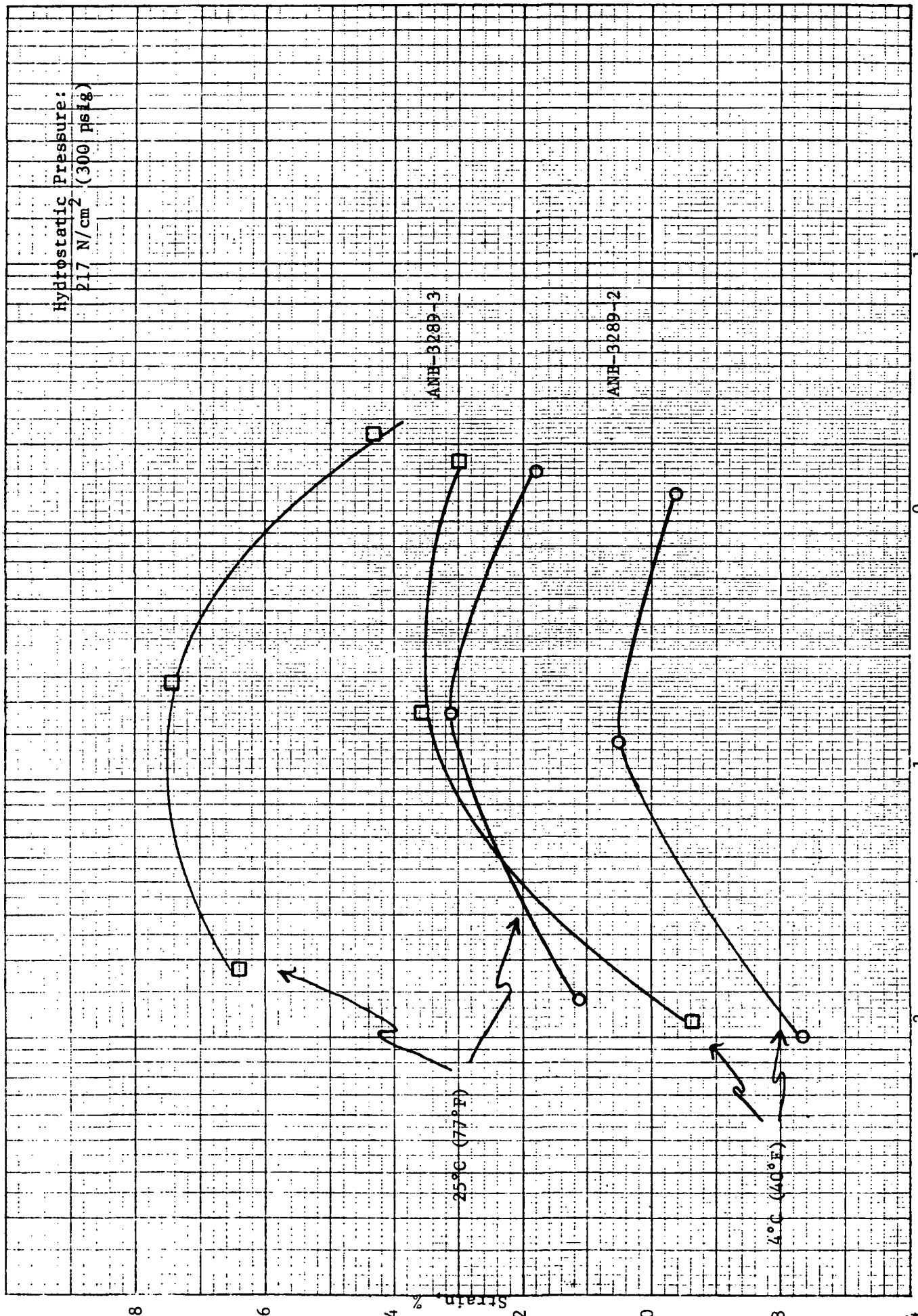

Figure 13

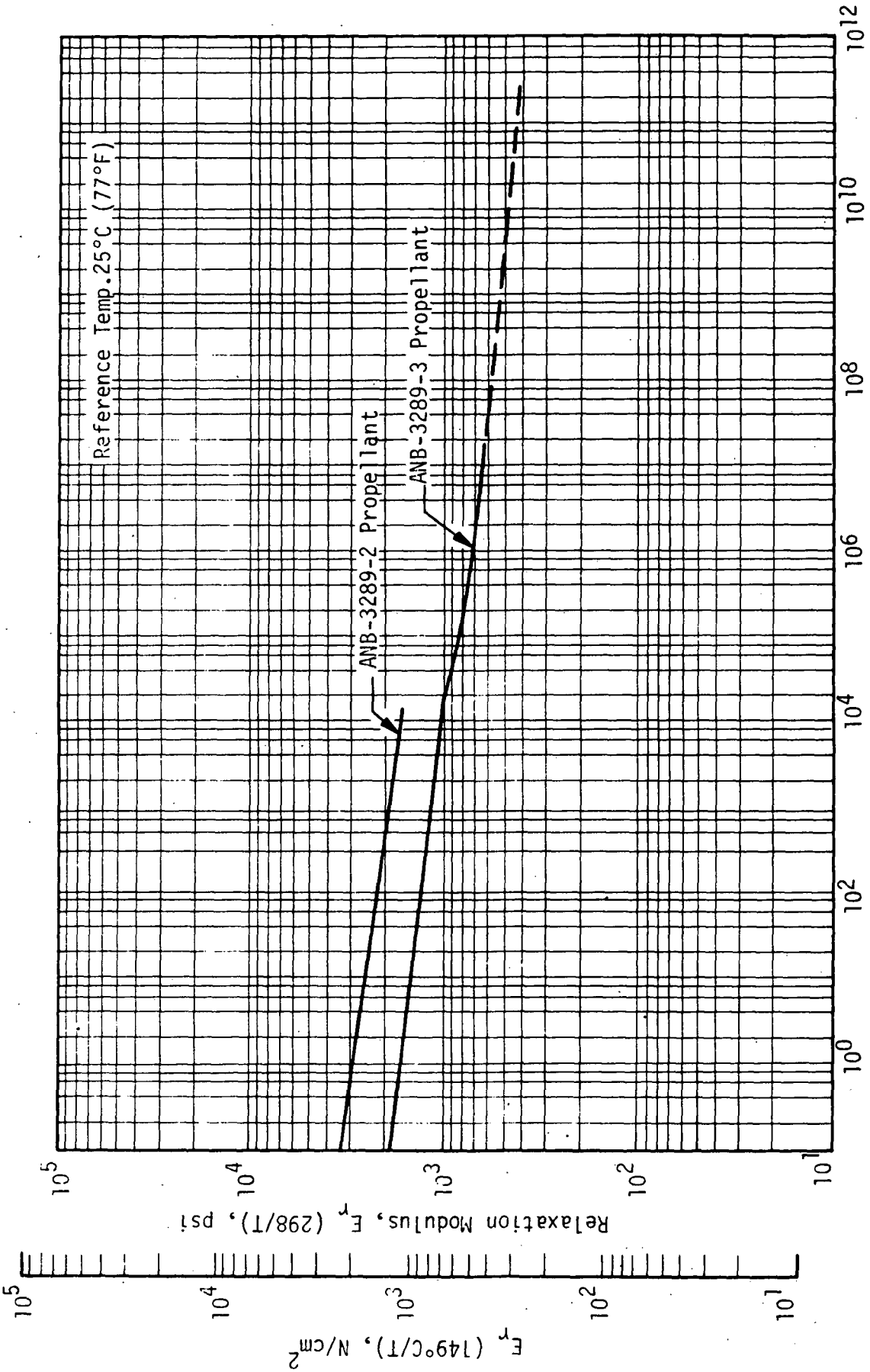

Master Relaxation Curve for ANB-3289 Propellant Modifications

Figure 14

since been traced to a softening of plexiglass end plates used in the previous test. Tests made using aluminum end plates gave a normal relaxation curve, hence the data for ANB-3289-2 above 93°C (200°F) where the discontinuity occurred is not shown. Time temperature shift plots for the two propellants are presented in Figure 15. The ANB-3289-2 propellant plot has been extended as if no discontinuity had occurred.

Constant rate shear measurements on poker chip specimens of ANB-3289-3 propellant from batch 71-63 bonded to SD-886 liner and Gen-Gard V-4030 insulation were conducted at 25, 65, 93 and 135°C (77, 150, 200 and 275°F) using crosshead rates of 5.1, 0.51 and 0.051 cm/min (2.0, 0.2 and 0.02 in./min). The shear values obtained, time to failure and failure mode are given in Figure 16. Again, the difficulty of assuring primary bond failure is evidenced by the secondary bond failures occurring at 25, 65 and 93°C (77, 150 and 200°F). These values therefore represent minimums. Specimens evidencing secondary bond failure were rebonded using a grooved propellant surface and retested at 25°C (77°F). These results are shown in Figure 17. These specimens failed in cohesive failure either in the propellant away from the bond interface (CP) or near the interface (CPI). The bond shear values, however, were not too significantly different from those obtained previously. Plots of the effect of shear stress on time to failure for poker chip specimens of ANB-3289-3 and ANB-3289-2 are shown in Figure 18. A master curve showing time shifted data is presented in Figure 19.

The effect of strain rate on the bond shear strength of poker chips prepared with ANB-3289-3/SD-886 liner/Gen-Gard V-4030 insulation under 217 N/cm^2 (300 psig) pressure is shown in Figure 20. Comparative plots for ANB-3289-3 and ANB-3289-2 are shown in Figure 21.

Constant bond tensile measurements conducted with similar poker chip specimens of ANB-3289-3 propellant/SD-886 liner/Gen-Gard V-4030 insulation were made at -18, 25 and 65°C (0, 77 and 150°F) at crosshead rates of 5.1, 1.3, 0.51 and 0.051 cm/min (2.0, 0.5, 0.2 and 0.02 in./min). The tensile values, time to failure and failure mode are given in Figure 22. These specimens had sleeve type bonds for secondary bonds insuring failure in the primary mode. Plots of these data and those previously obtained with ANB-3289-2 propellant are compared in Figure 23.

Time-Temperature Shift Factor for ANB-3289 Propellant Modifications

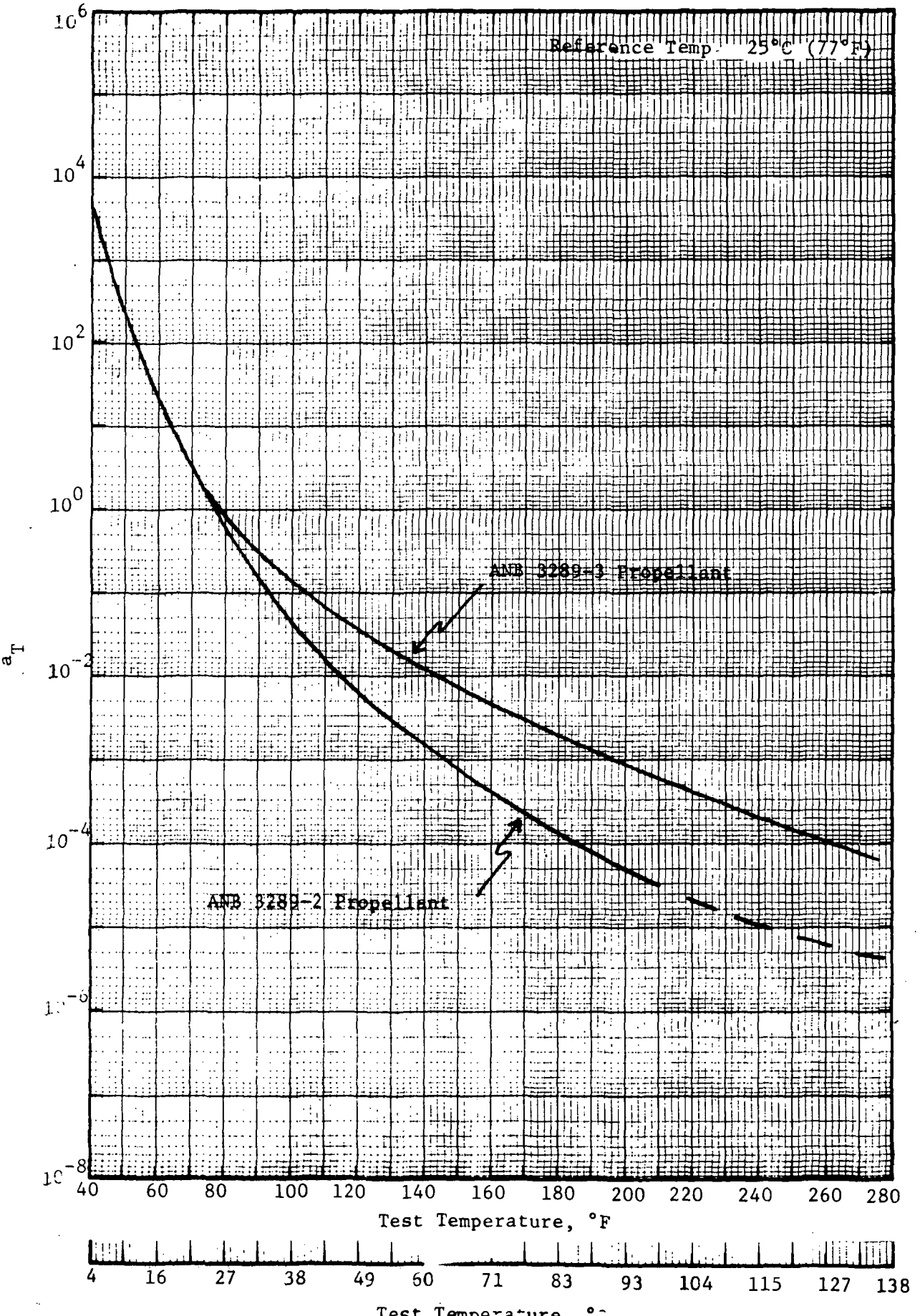

Figure 15

Aerojet Solid Propulsion Company

EFFECT OF TEMPERATURE AND CROSS HEAD RATE ON THE SHEAR STRENGTH OF ANB-3289-3 PROPELLANT BONDS - BATCH 71-63

(ANB-3289-3/SD-886/V-4030)

Test Temp., °C(°F)	Cross Head Rate, cm/min (in./min)	Stress, N/cm^2 (psi)	Time, min.	Mode of Failure(1), % CP	CPI	F
25 (77)	5.1 (2.0)	106 (154)	0.033	-	-	100
		112 (163)	0.042	-	-	100
	0.51 (0.2)	80 (116)	0.282	-	-	100
		90 (131)	0.294	-	-	100
	0.051 (0.02)	63 (92)	2.00	-	-	100
		60 (87)	1.50	-	-	-
65 (150)	5.1 (2.0)	59 (86)	0.025	-	-	100
		61 (89)	0.033	-	-	100
	0.51 (0.2)	50 (72)	0.270	-	-	100
		48 (70)	0.272	-	-	100
	0.051 (0.02)	37 (54)	2.4	-	-	100
93 (200)	5.1 (2.0)	41 (60)	0.0245	-	-	100
		53 (77)	0.03	-	50	50
	0.51 (0.2)	34 (50)	0.25	-	-	100
		32 (47)	0.22	-	-	100
	0.051 (0.02)	30 (44)	2.15	-	-	100
		26 (38)	2.44	-	-	100
135 (275)	5.1 (2.0)	31 (45)	0.021	-	100	-
		30 (43)	0.021	-	70	30
	0.51 (0.2)	20 (29)	0.21	-	100	-
		23 (34)	0.27	-	100	-
	0.051 (0.02)	19 (27)	2.6	-	100	-
		19 (27)	2.65	-	100	-

(1) CP - Cohesive failure in propellant
CPI - Cohesive failure in propellant within 1 mm of bond interface
F - Secondary bond failure.

Figure 16

RETEST OF SHEAR SPECIMENS

Test	Test Temp., °C (°F)	Cross-Head Rate cm/min (in./min)	Stress N/cm^2 (psi)	Time, min	Mode of Failure, %(1) CP	CPI	F
Constant Rate Shear	25 (77)	0.051 (0.02)	59 (86)	4.9	100	-	-
(Rerun of specimens which failed at secondary bond)			65 (94)	2.7	100	-	-
		0.51 (0.2)	68 (98)	0.5	100	-	-
			88 (127)	0.37	-	100	-
		5.1 (2.0)	127 (184)	0.051	100	-	-
			125 (181)	0.047	50	50	

(1) CP - Cohesive failure in propellant.
CPI - Cohesive failure in propellant within 1 mm of bond interface.
F - Secondary bond failure.

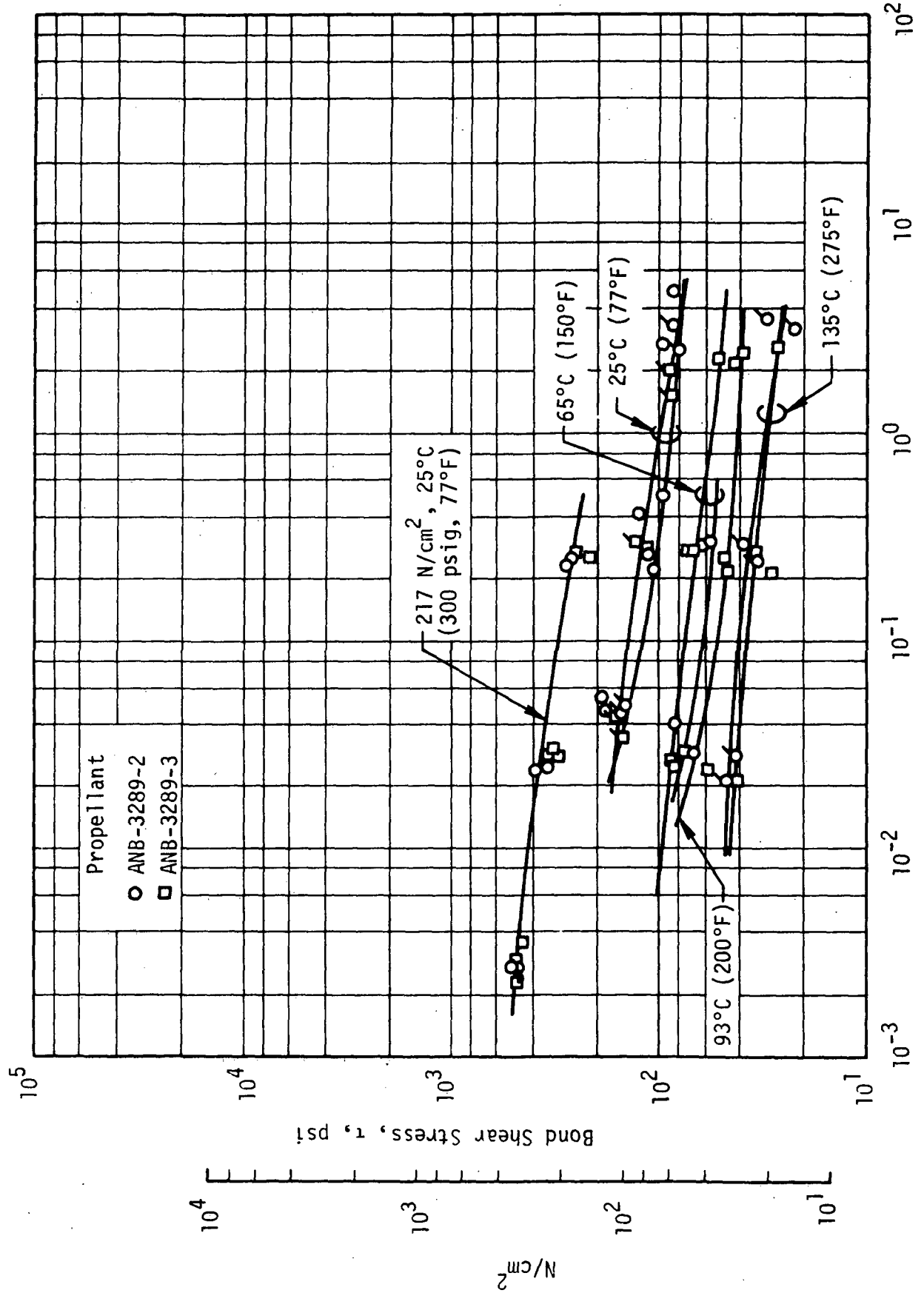

Effect of Bond Shear Stress on Time to Failure, ANB-3289 Propellant Modifications

Figure 18

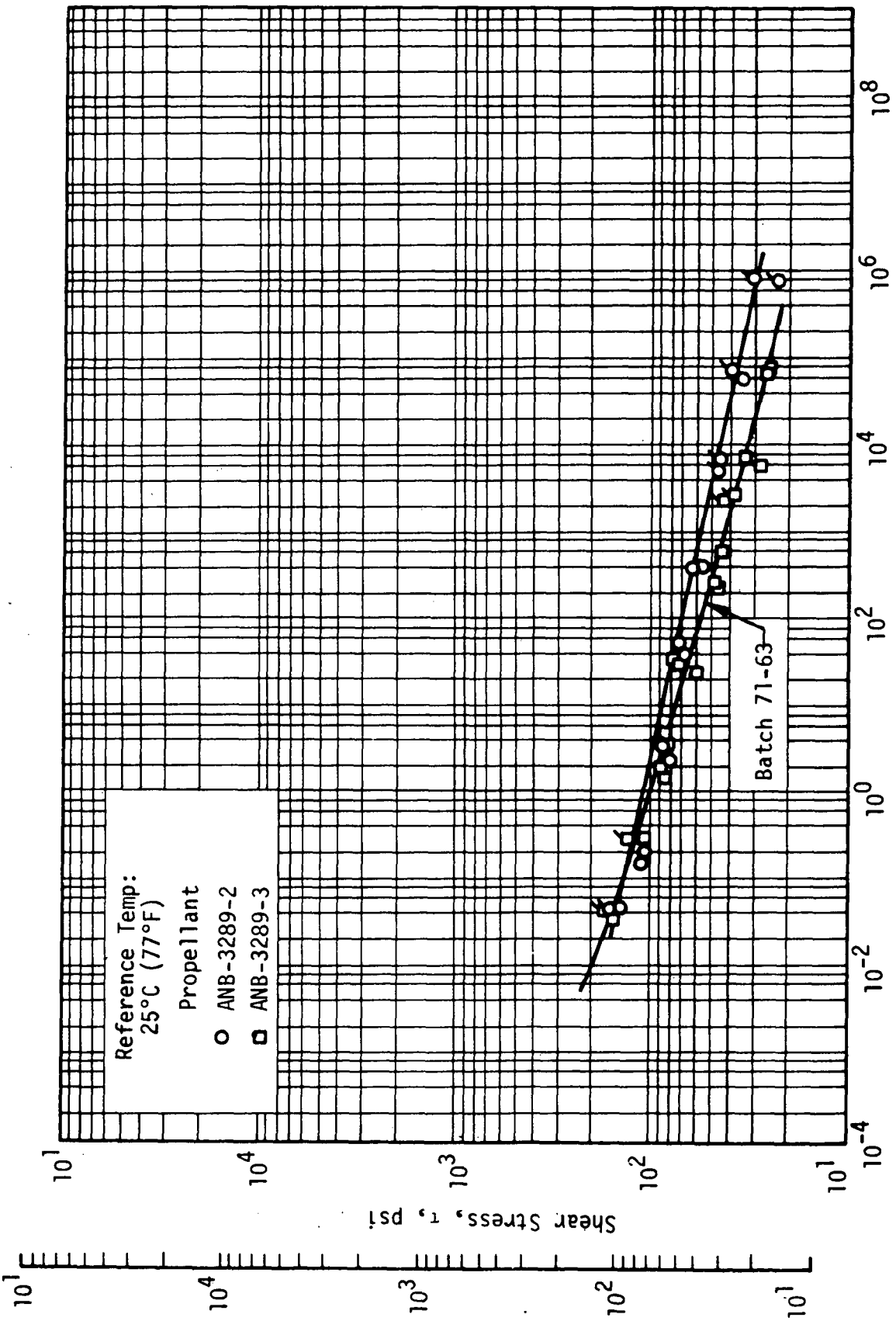

Effect of Bond Shear Stress on Reduced Time-to-Failure for ANB-3289 Propellant Modifications (ANB-3289/SD-886/V-4030)

Figure 19

EFFECT OF STRAIN RATE ON BOND SHEAR STRENGTH OF
ANB-3289-3 UNDER PRESSURE 217 N/cm^2 (300 psig)

(ANB-3289-3/SD-886/V-4030)

Test	Test Temp., °C (°F)	Strain Rate, $min.^{-1}$	Stress N/cm^2 (psi)	Time, sec	Mode of Failure, %(1) CP	CPI	F
High Rate Shear	25 (77)	5	157 (228)	15.0	-	-	100
			176 (255)	15.8	-	-	100
			176 (255)	16.5	-	-	100
		50	215 (312)	1.7	-	-	100
			228 (331)	1.7	-	-	100
			228 (331)	1.8	-	-	100
		500	343 (498)	0.17	-	-	100
			325 (471)	0.21	-	-	100
			334 (484)	0.14	-	-	100

(1) CP - Cohesive failure in propellant
CPI - Cohesive failure in propellant within 1 mm of bond interface
F - Secondary bond failure

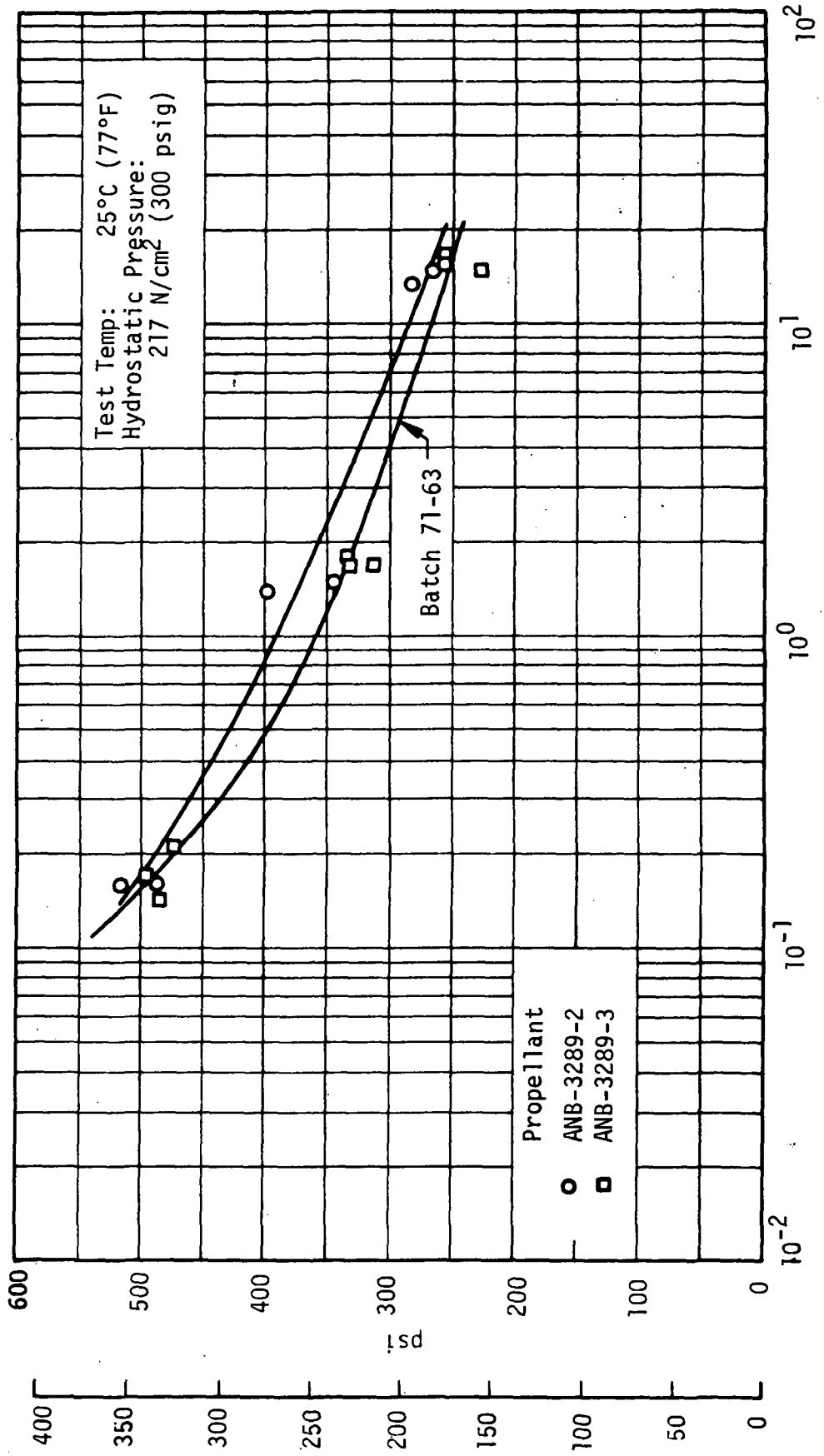

The Effect of Maximum Shear Stress on Time-to-Failure Under Pressure (Propellant/SD-886/V-4030)

Figure 21

BOND TENSILE STRENGTH

(ANB-3289-3/SD-886/V-4030)

Test	Test Temp., °C (°F)	Cross-Head Rate cm/min (in./min)	Stress, N/cm^2 (psi)	Time, min	Mode of Failure, %(1) CP	CPI
Constant Rate Tensile (sleeved)	-18 (0)	0.051 (0.02)	710 (1030)	4.60	100	-
			786 (1140)	5.20	100	-
		0.51 (0.2)	1007 (1460)	0.450	100	-
			951 (1380)	0.510	100	-
		5.1 (2.0)	1151 (1670)	0.0541	100	-
			1207 (1750)	0.0530	20	80
	25 (77)	0.051 (0.02)	92 (134)	1.9	50	50
			70 (101)	1.7	20	80
		0.51 (0.2)	114 (166)	0.195	5	95
			130 (189)	0.229	2	98
		1.3 (0.5)	128 (186)	0.096	2	98
			126 (183)	0.090	-	100
		5.1 (2.0)	164 (238)	0.030	-	100
			156 (226)	0.023	5	95
	65 (150)	0.051 (0.02)	47 (68)	1.65	-	100
			45 (65)	1.43	5	95
		0.51 (0.2)	35 (51)	0.195	-	100
			62 (90)	0.238	-	100
		5.1 (2.0)	105 (153)	0.0295	-	100
			94 (136)	0.023	-	100

(1) CP - Cohesive failure in propellant.

CPI - Cohesive failure in propellant within 1 mm of bond interface.

Figure 22

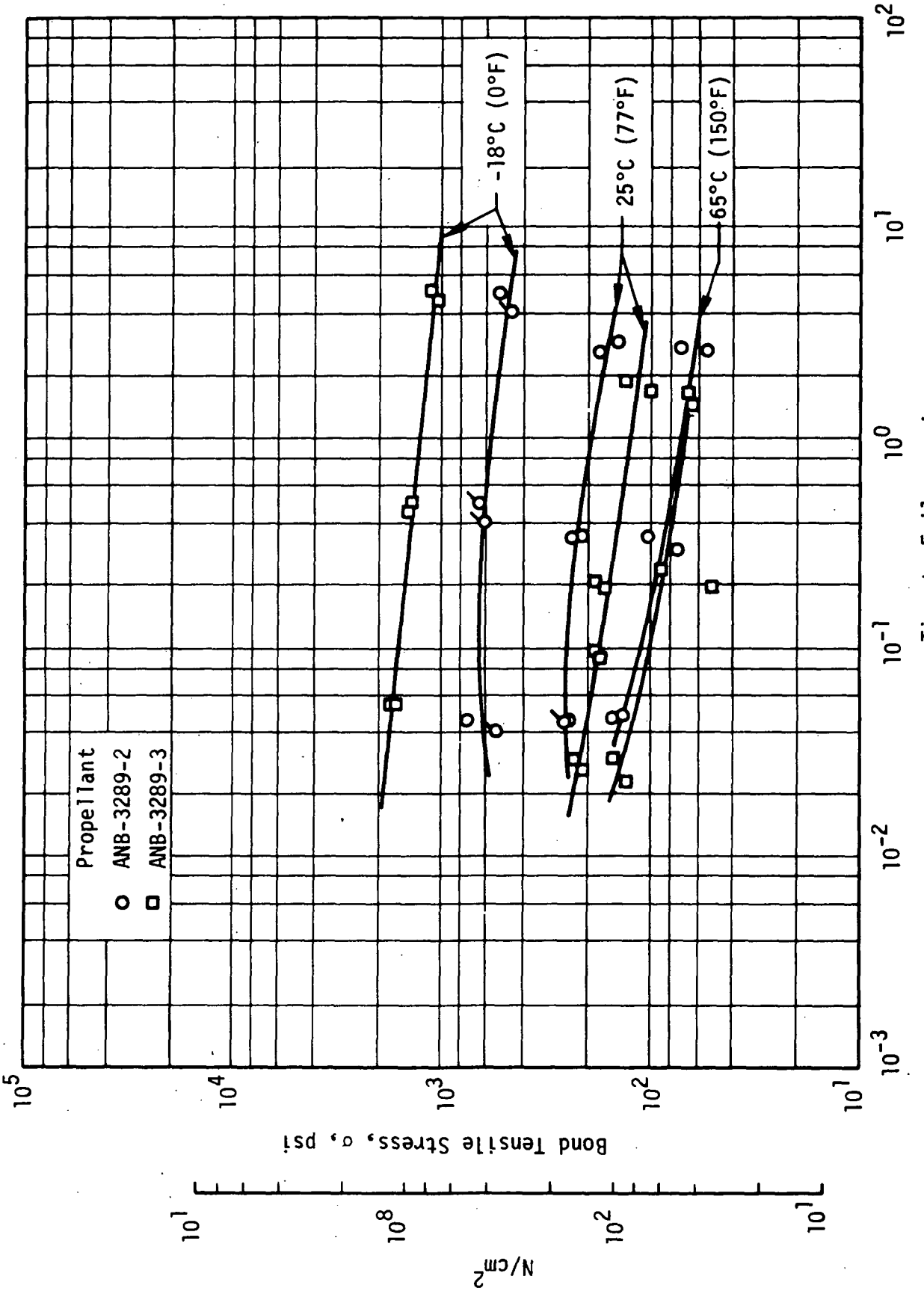

The Effect of Bond Tensile Stress on Time-to-Failure for ANB-3289 Propellant/SD-886/V-4030 Poker Chip Specimens

Figure 23

Master curves showing time shifted data are presented in Figure 24.

The coefficient of thermal expansion for ANB-3289-3 propellant (Batch No. 71-63) was measured by a volumetric method over the temperature range 4 to 112°C (40 to 232°F). The volumetric coefficient of thermal expansion (β) was found to be 3.28×10^{-4} $m^3/m^3/°C$ (1.82×10^{-4} $in.^3/in.^3/°F$). This on conversion gives a linear coefficient of thermal expansion (α) of 10.9×10^{-5} m/m/°C (6.1×10^{-5} in./in./°F). This value is in close agreement with those obtained by a linear method for ANB-3289-2 propellant.

Samples of ANB-3289-3 propellant were tested at Aerojet Solid Propulsion Company for conformance to the requirements of the ICC classification "B". These data are shown in Figure 25. Propellant was also shipped to Bureau of Explosives testing laboratory where the Class "B" rating was confirmed.

C. HEAT STERILIZATION OF ANB-3289-3 PROPELLANT

To confirm the stability of the propellant raw material lots selected for the motor program to heat sterilization, two 7.5 x 7.5 x 12.5 cm (3 x 3 x 5 in.) blocks of ANB-3289-3 propellant from batch 71-63 were subjected to heat sterilization cycles at 135°C (275°F). One block was removed after one cycle of 56 hrs at 135°C (275°F) and tested for burning rate and mechanical properties. The second block of propellant was subjected to the full six cycles prior to testing burning rate and mechanical properties.

Solid strand burning rate data was obtained for each block of sterilized propellant. Figure 26 shows these data which indicate no change in solid strand burning rate was experienced due to heat sterilization.

Mechanical properties test data obtained from the two blocks of propellant are tabulated in Figure 27. Although there was a slight indication of hardening after one sterilization cycle, the trend was not prevalent through the six cycles. The data from six cycles are identical with the initial non-cycled mechanical properties. These data confirm previous conclusions based on 10-lb

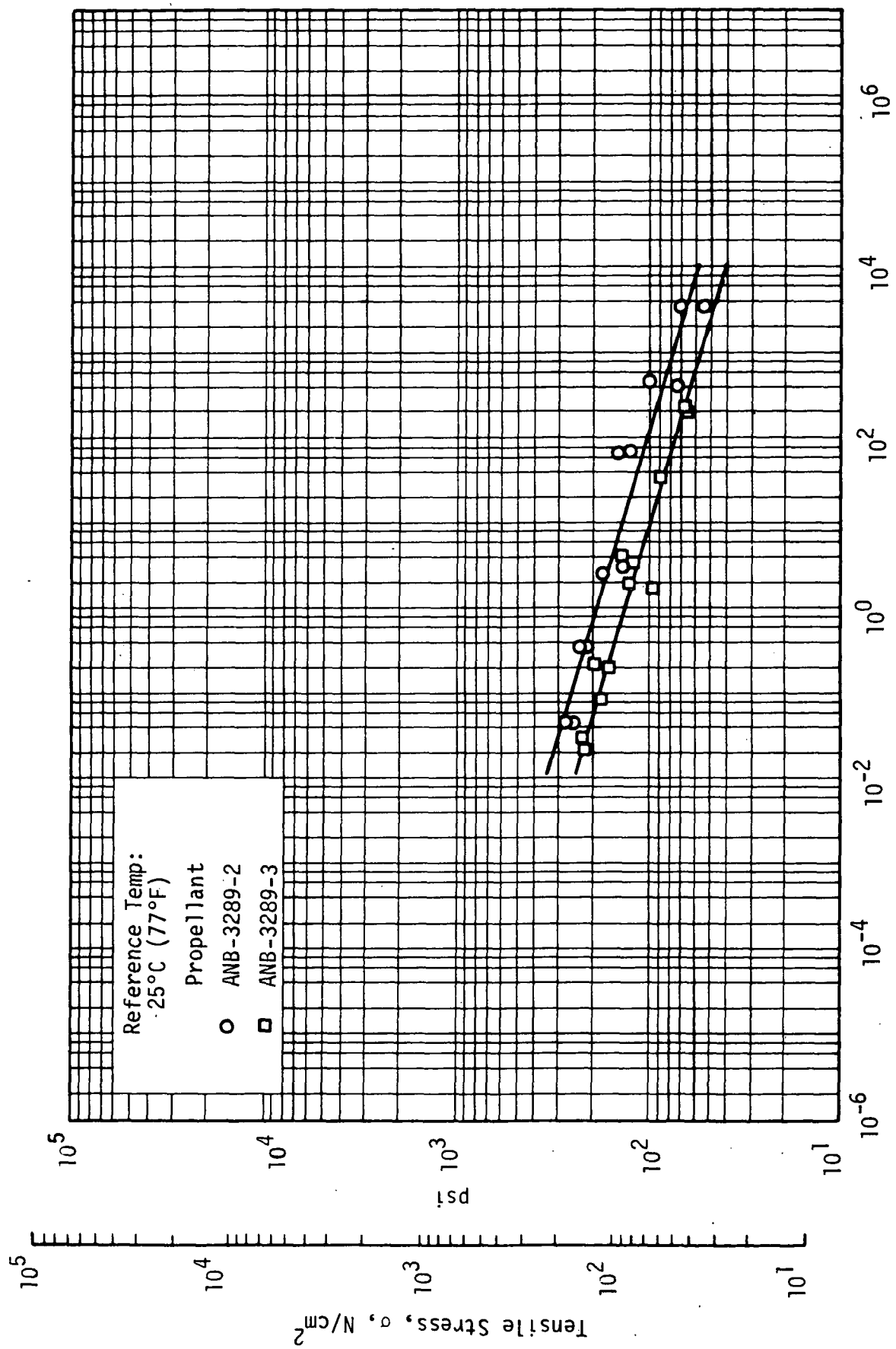

Effect of Tensile Stress on Time-to-Failure of ANB-3289-2 and ANB-3289-3 Propellant-to-Liner Bonds

Figure 24

ICC CLASSIFICATION TESTING FOR ANB-3289-3 PROPELLANT

A.	5.1 cm (2-inch) cube with No. 8 blasting cap (4 tests)	Negative
B.	5.1 cm (2-inch) cube with engineer's special blasting cap (4 tests)	Negative
C.	Ignition and unconfined burning tests:	
	2.5 cm (1-inch) cube (1 test)	Burned 15 sec.
	5.1 cm (2-inch) cube (2 tests)	Burned 26 sec.
	4-5.1 cm (2-inch) cube (1 test)	Burned 26 sec.
D.	Thermal stability test (48 hours at 75°C) 5.1 cm (2-inch) cube (1 test)	No change
E.	Autoignition test, °C (°F)	330 (625)
F.	Impact sensitivity cm/2Kg*	15.4
G.	Bureau of Explosives Classification	"B"

* Not I.C.C. test

Figure 25

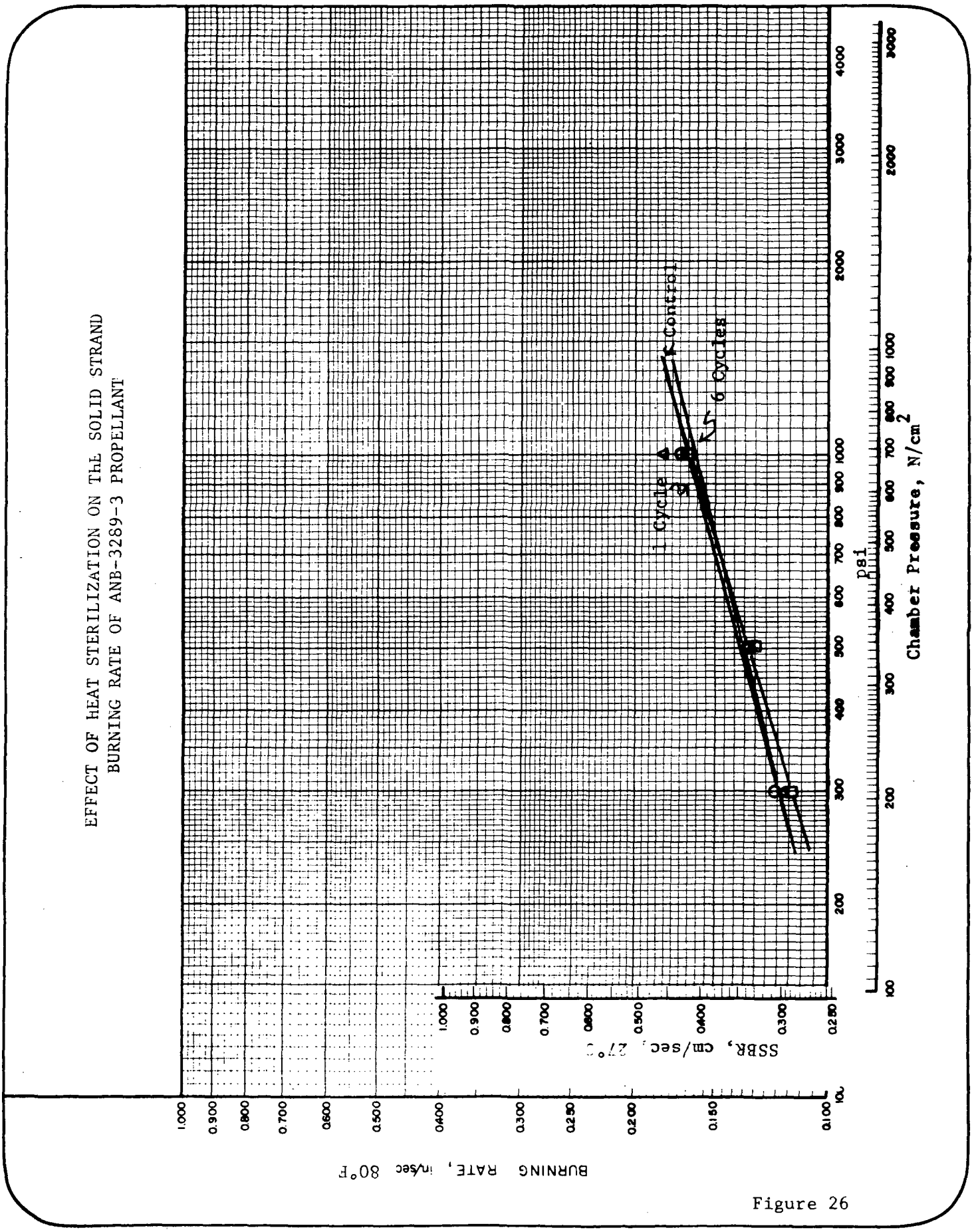
EFFECT OF HEAT STERILIZATION ON THE SOLID STRAND
BURNING RATE OF ANB-3289-3 PROPELLANT
BURNING RATE, in/sec 80°F
SSBR, cm/sec, 27°C
Chamber Pressure, N/cm2
psi
1 Cycle
6 Cycles
Control

Figure 26

EFFECT OF HEAT STERILIZATION ON THE UNIAXIAL TENSILE PROPERTIES OF ANB-3289-3 PROPELLANT

No. of Sterilization Cycles[1]	Mechanical Properties at 25°C (77°F)[2] σ_m N/cm^2 (psi)	ε_m %	ε_b %	E_o N/cm^2 (psi)	Shore "A" Hardness
0	106 (154)	14	20	1138 (1650)	68
1	114 (165)	13	14	1344 (1950)	75
6	102 (148)	15	20	1117 (1620)	72

(1) Each cycle - 56 hours at 190°C (275°F)

(2) Strain rate 0.74 min.$^{-1}$

laboratory scale propellant mixes and indicate the raw materials selected for use in the motor demonstration program are completely acceptable.

D. STRESS-FREE TEMPERATURE DETERMINATION

1. Basis for Tests

A test program was devised to define the effect of sterilization on stress-free temperature T_{sf}. This definition is critical to the grain stress analysis. The basic premise of past studies was that T_{sf} changes occur by the breaking and reformation of polymeric chains in the propellant binders; the chain failures being induced by mechanical loads. However, underlying this premise is the assumption that the crosslinked network constitutes the basic feature of structural permanence. The test program provides a test of this assumption for the sterilization temperature region.

2. Test Plan

Testing was designed to evaluate T_{sf} by two approaches, strain recovery and stress relaxation measurements. The specimen used here was 5.08 cm (] in.) dia x 12.7 cm (5 in.) long with metal plates bonded to both ends. Two sets of test specimens were used. One set provided all the data required for the strain recovery tests, while both sets were required for the stress testing. The first set of specimens was placed under a 5% compression and exposed to the sterilization thermal cycles; while the second set was exposed unstrained.

At the end of the 1st, 3rd and 6th sterilization periods the strained specimens were released while still at 135°C. Then both sets of specimens were cooled to 25°C where their recovery was monitored for about 72 hours. After the 1st and 3rd cycles the pre-strained specimens were returned to their previous deformations and both sets were, again, placed in the oven for further sterilization cycling.

After the 6th heating cycle, recovery of the specimens was monitored for about 10 days. Then they were machined (to give a smaller cross-section except for the flanged ends which were required to prevent bond failures) and tested in stress relaxation.

3. Strain Recovery Test Results

The new stress-free temperature, T_{sfn}, is related to the high storage temperature, T_h, as follows:

$$T_{sfn} = T_{sfo} + f\ (T_h - T_{sfo})$$

where T_{sfo} is the original stress-free temperature and f is a factor obtained from the change in shape during high temperature storage

Values of f are shown in Figure 28. Each reported value is the average of three length measurements.

As shown, the values of f (hence, of T_{sfn}) increase with the number of sterilization cycles. The following tabulation summarizes these changes:

Heat Sterilization Cycle	Average Values of f	T_{sfn}, °C (°F)	
1	0.824	121	(250)
3	0.909	128	(262)
6	0.935	130	(266)

The near equilibrium character of the strain recovery measurements are shown in Figure 29 in a graph of the average values of f versus the recover time.

VALUES OF f AS MEASURED IN STRAIN

RECOVERY AT 25°C (77°F)

Spec. No.	After 1st Sterilization Cycle		After 3rd Sterilization Cycle				After 6th Sterilization Cycle			
	Recovered 18.5 Hrs	Recovered 56 Hrs	Recovered 8 Hrs	Recovered 25 Hrs	Recovered 49 Hrs	Recovered 73 Hrs	Recovered 5 Hrs	Recovered 101 Hrs	Recovered 197 Hrs	Recovered 317 Hrs
2	0.817	0.825	0.890	0.899	0.900	0.900	0.934	0.941	-	-
3	0.824	0.831	0.895	0.904	0.904	0.904	0.933	0.940	0.937	0.937
4	0.814	0.822	0.889	0.898	0.902	0.902	0.938	0.944	0.936	0.945
5	0.833	0.773	0.892	0.903	0.902	0.901	0.934	0.937	0.936	0.940
6	0.851	0.856	0.844	0.856	0.856	0.856	0.879	0.878	0.884	0.888
7	0.814	0.821	0.905	0.915	0.915	0.916	0.928	0.943	0.946	0.941
8	0.848	0.854	0.903	0.912	0.908	0.914	0.948	0.954	0.952	0.956
9	0.840	0.841	0.846	0.849	0.850	0.849	0.909	0.922	0.923	0.928
10	0.775	0.789	0.826	0.830	0.829	0.829	0.936	0.926	0.939	-
11	0.828	0.832	0.935	-	1.006	0.944	0.935	0.941	0.940	0.946

VALUES OF f AS MEASURED IN STRAIN RECOVERY
AFTER 6TH STERILIZATION CYCLE

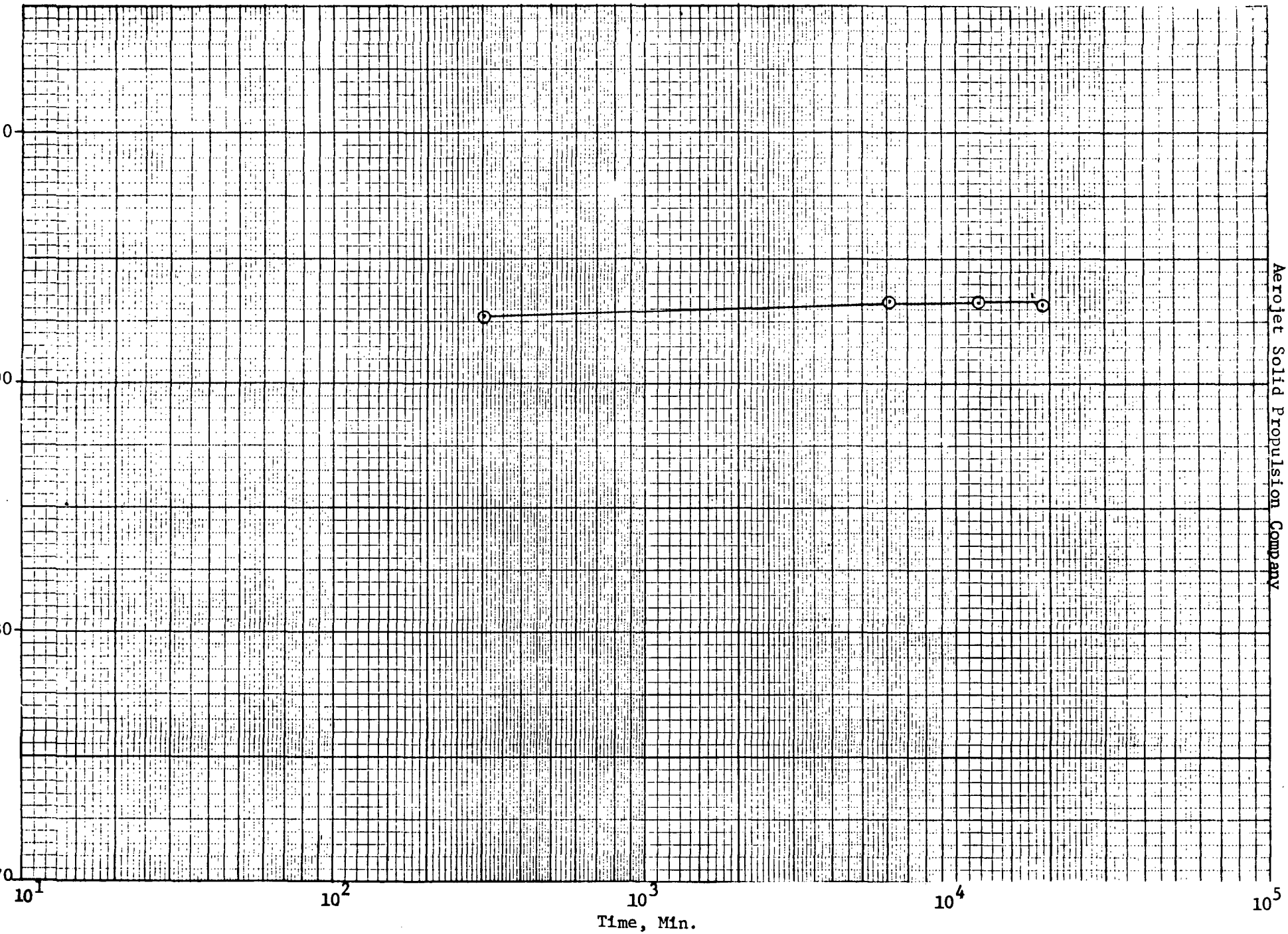

Figure 29

4. Results of Stress Relaxation Tests

In this test, one set of specimens was stored at T_h without load; while the second set of specimens was placed under a 5% compression and stored at T_h for the required periods. At the end of each period the specimens were unloaded and returned to room temperature and thermally equilibrated.

At this point, the two sets of specimens were tensile strained about 1% and the tensile stresses monitored as in a stress relaxation test. The two relaxation curves appear roughly as shown below.

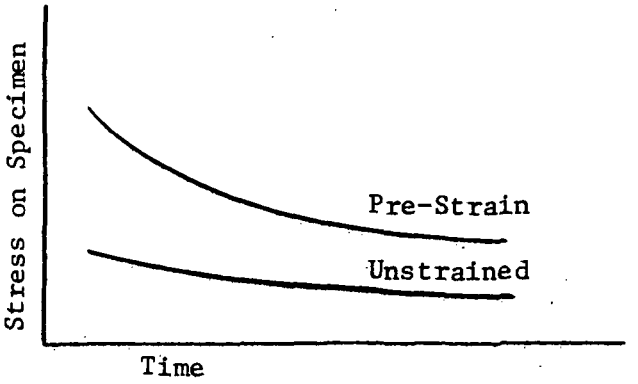

For these tests, the factor f is computed from the following:

$$f = \frac{\varepsilon_t - \frac{\sigma_s}{E_e}}{\varepsilon_h \left(1 + {}^{\sigma}s/E_e\right)}$$

where σ_s is the stress on the prestrained specimen

E_e is the equilibrium modulus

ε_t is the test strain level, based on the original dimensions,

ε_h is the pre-strain imposed during sterilization

The value of E_e was estimated from tests on the unstrained specimens. These values, along with the specified values of σ_u and ε_u, are listed in Figure 30 for stress relaxation testing at 25°C (77°F) for 100 minutes. The average modulus was found to be 994 N/cm^2 (1440 psi).

The values of ε_t, ε_h, and σ_s, after 100 minutes at 25°C (77°F) given in Figure 31 for the pre-strained specimens. The values of f were computed and reported in Figure 31.

The average value of f was found to be 0.950, which corresponds to a T_{sfn} of 131°C (268°F). This is in good agreement with the strain recovery data where an average value of 130°C (266°F) was obtained.

5. Additional Tests

The extent of the changes shown in these measurements was considerable and much more than was expected. Therefore, it was concluded that the changes must occur for reasons which are not associated with chemical crosslinking. Accordingly, further investigations were initiated.

The effects explored here attempted to define (not rigorously) the effects of: (1) simultaneous cooling and straining; (2) the permanence of the stress-free temperature change; and (3) the effect of strain level. In these test efforts only strain recovery measurements were made.

a. Specimen No. 21

In this testing a fresh propellant specimen (No. 21) was clamped in the strain fixture at 0% strain at 250°C, then placed in the sterilization oven. On heating, a compressive thermal strain of 1.01% was produced in the specimen. After the sterilization cycle the specimen was held in the fixture while the oven cooled to room temperature (about 8 hours). To insure thermal equilibration, the specimen was removed from the restraining fixture and the recovery followed with time.

STRESS RELAXATION TESTING AT 25°C (77°F) OF UNSTRAINED SPECIMENS AFTER 6 STERILIZATION CYCLES

SPECIMEN NO.	STRAIN, %	STRESS AT 100 MIN		MODULUS AT 100 MIN	
		N/cm^2	(psi)	N/cm^2	(psi)
14	1.03	11.4	(16.5)	1105	(1600)
15	2.03	16.3	(23.6)*	800	(1160)
16	1.96	18.8	(27.2)	959	(1390)
17	1.03	12.8	(18.5)	1236	(1790)
18	2.88	25.3	(36.6)	876	(1270)
			Mean =	994	(1440)

* By extrapolation of 10 minute data.

STRESS RELAXATION TESTING AT 25°C OF PRE-STRAINED
SPECIMENS AFTER 6 STERILIZATION CYCLES

SPECIMEN NO.	PRE-STRAIN, %	ε_t, %	STRESS AT 100 MIN		f
			N/cm^2	(psi)	
3	-6.33	-5.10	10.1	(14.7)	0.955
4	-6.46	-4.39	15.8	(22.9)	1.058
5	-6.59	-4.54	16.8	(24.3)	0.930
6	-6.85	-4.19	15.1	(21.9)	0.820
7	-5.96	-4.90	9.2	(13.3)	0.967
8	-6.66	-5.55	9.5	(13.8)	0.968
9	-6.53	-5.42	10.5	(15.2)	0.982
10	-6.27	-3.47	19.5	(28.3)	0.850
11	-6.34	-5.43	10.8	(15.6)	1.018
				Mean =	0.950

Figure 31

The values of f obtained were about 70% of those observed for the first cycle recovery data in the initial test measurements.

b. Specimen No. 10

No fresh propellant was available for this test, so a previously tested specimen, No. 10, was used. The specimen, in the straining fixture, was placed under a tensile strain of 1.01% at 25°C. Then it was heated to 135°C where the thermal compressive strain offset the tensile strain. Thus, with essentially no imposed strain at 135°C the sample had no basis for changing its shape; hence, the stress-free temperature should not change.

At the end of the sterilization cycle the specimen was kept in the straining fixture while the oven cooled to 25°C (about 8 hours). After thermal equilibration the restraint was removed and the recovery was monitored.

As shown in Figure 32, the values of f decrease with the time. This behavior suggests that the shape of the specimen after the initial tests was, indeed, permanent -- since the specimen is asymptotically returning to that length. This is also supported by the reversed direction of the graph of f versus log time.

This latter effect is attributed to the fact that the change in f could only occur during the cooling step where the specimen experiences simultaneous cooling and straining. That is, as the specimen cools it develops tensile strains. The tensile strains cause plastic flow, with the greatest flow occurring at high temperatures and high strains. But, in this test the strains are low at the high temperatures and high at the low temperatures. Therefore, we should expect only a partial shift in the values of f, as observed.

c. Specimen No. 5

Specimen No. 5 (previously tested) placed in 1.0% compression and subjected to a new sterilization cycle with a total compressive strain of 2.07%. After the heat cycle the specimen was held in the strain fixture until thermal equilibration (about 28 hours), then monitored in recovery.

EFFECT OF SIMULTANEOUS COOLING AND STRAINING ON MEASUREMENTS
OF f IN STRAIN RECOVERY AT 25°C (77°F) (SPECIMEN HELD AT 0% STRAIN AT 135°C)

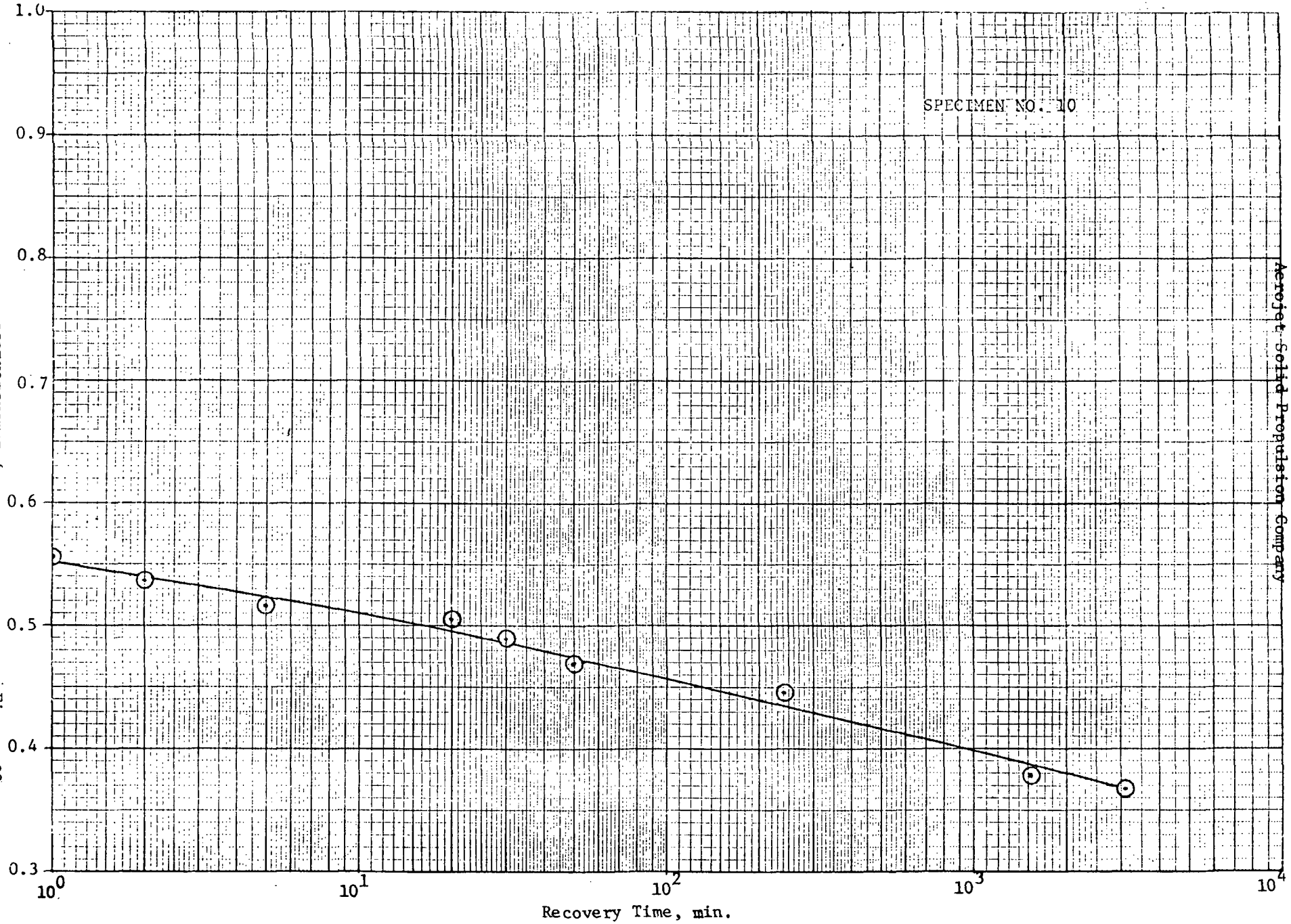

Figure 32

As shown in Figure 33, there is a marked change in f from the initial tests, with only slight time dependence in recovery. This indicates the propellant had permanently changed its shape during the previous treatment, and the subsequent change in shape appears permanent.

The difference between this result and those for the first cycle of the initial tests is believed to be due to the simultaneous cooling and straining effects imposed on specimen No. 5 after the heat cycle.

d. Specimen No. 20

Specimen No. 20 was held under 0% strain at 25°C and heated to 135°C where a thermal compressive strain of 1.08% was obtained. This test is identical to the one imposed on the fresh propellant specimen No. 21.

Specimens 20 and 21 minimize the effects of simultaneous cooling and straining while emphasizing the change in shape under thermal strains at the high temperature. The reason for the greater change in shape of specimen No. 20 (Figure 33) is probably related to the stresses produced by the higher modulus in this specimen. (The modulus increased about 16 to 20% after six sterilization cycles which is not consistent with other data.)

e. Comparison of Tests

The observed behaviors from these four tests, and the previous first cycle initial tests, are summarized in the following tabulation:

	IMPOSED STRAINS, %				
	No. 10	No. 21 (Fresh Propellant)	No. 20	No. 5	Initial Tests (Unloaded at 135°C)
25°C	+1.0	0	0	-1.0	-5
135°C	0	-1.01	-1.08	-2.07	-6

Observed Recovery Curves: f

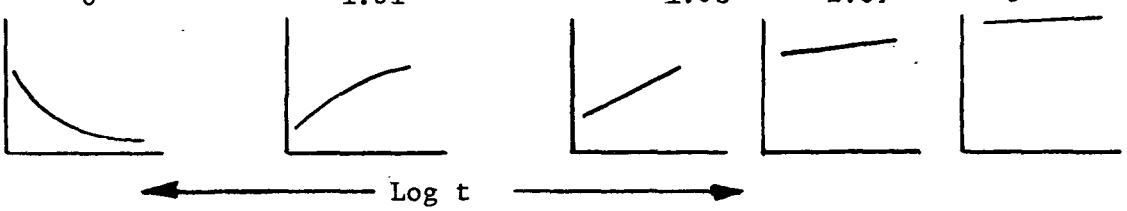

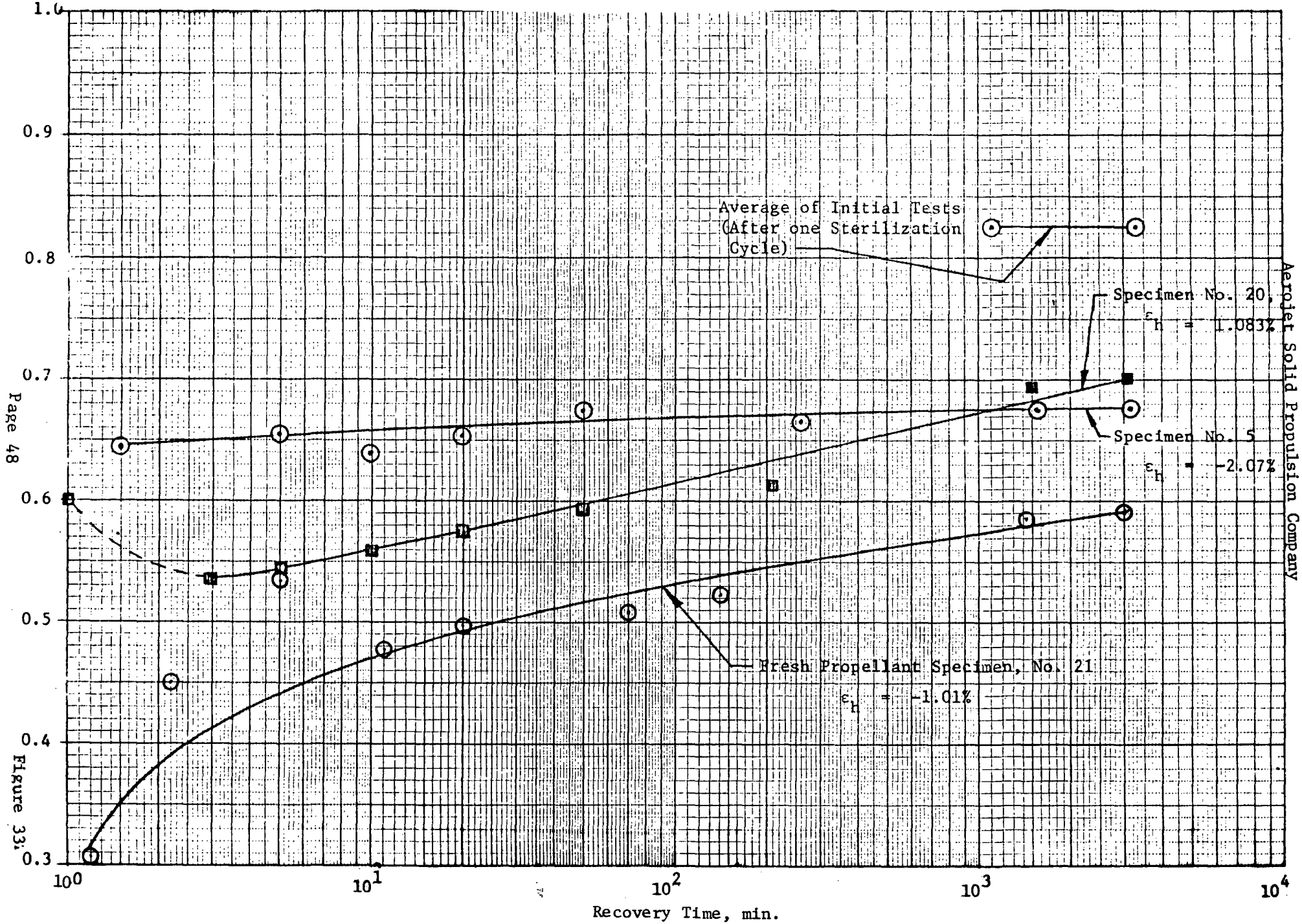
1.6
0.9
0.8
0.7
0.6
0.5
0.4
0.3
Average of Initial Tests (After one Sterilization Cycle)
Specimen No. 20, ε_h = 1.083%
Specimen No. 5 ε_h = -2.07%
Fresh Propellant Specimen, No. 21 ε_h = -1.01%
10^0
10^1
10^2
10^3
10^4
Recovery Time, min.
Aerojet Solid Propulsion Company

Figure 33

This tabulation gives an ordered progression of the imposed strains, both at 25°C and 135°C. The progression is reflected in the shapes of the recovery curves. As the strains become more compressive they change slope; being negative in the tensile strain region and positive in the compressive strain region. Also, the magnitude of the recovery values increases with the compressive strain.

6. Interpretation of Observed Processes

The behavior involved here, in its simplest sense, may be described as a recovery process after a period of loading. During the loading phase work is done against the damping elements of the retarded elasticity, rather than against the elastic element. In the case of extremely high viscosity and low modulus (as obtained in all composite propellants) this behavior can hardly be distinguished from a true flow, which results in permanent set.

At this point it is not certain that there is "true" flow in the propellant. That is, a change in shape of the specimen such that it can never return to its original condition. The behavior may be one in which the viscosity is so high that the elastic element can induce only extremely slow changes in the shape. In a complex loading path, such as exists here, the retarded elasticity processes can produce temporary shifts in the reference shape. Thus, the propellant may, for a time, appear to be recovering towards a new shape when, in actuality, its original shape remains the "true" reference condition; and given enough time (like 200 or 300 years) it might return to that shape.

7. Implications of Test Results

It is evident that, based on the initial series of tests, a high degree of shift in stress-free temperature can be encountered, given the right conditions. However, those specific conditions are not necessarily representative of the loads encountered with a case-bonded propellant grain, where the cycle of tensile or zero stress at low temperatures progressing to compression at high temperatures, and finally to increased tension at low temperatures.

The later tests showing the effects of different loading conditions (1) serve to show that the initial tests were unnecessarily severe and (2) give an indication of the nature of the phenomenon. However, these conditions do not necessarily represent motor conditions and cannot be used for design data. It is apparent that by careful manipulation of the thermal loads that potential tensile stresses induced during the post-sterilization cooling transient might be used to force the stress-free temperature down to a more acceptable level. This approach would have to be tailored to each specific motor configuration.

For the design requirements of this program, it must be assumed that a high degree of stress-free temperature shift will be encountered.

E. GRAIN DESIGN ANALYSIS

1. Objectives and Approach

The grain design task was to analyze two types of grain designs for the 45.0 cm (17.7 in.) dia SVM-3 motor case.

— A conventionally bonded grain using release boots if necessary.

— A thicker-web version using intermittent bonds (such as spots or strips) to provide relief of stresses and strains.

The technical approach was to start with a nominal case-bonded configuration and alter the dimensions (web thickness) until the critical stresses or strains were equal to or less than the allowables for the propellant and propellant-to-liner bond. Then various bond-release concepts were applied to maximize the web thickness. Conditions of storage at 21°C (70°F) for three months and static firing at 21°C (70°F) were considered for structural analysis purposes.

2. Method of Analysis

The structural analysis of the sterilizable motor grain was performed by means of finite element computer programs developed specifically for the analysis of solid propellant grains.(1) These programs are designed to handle two dimensional structures which can be either axisymmetric solids or arbitrary cross-sections under generalized plane strain or plane stress conditions. In the case of an axisymmetric structure the finite element approach replaces the continuous structure with a system of elastic quadrilateral rings (elements) that are interconnected at a finite number of nodal points (joints). The equilibrium equations, in terms of unknown nodal point displacements, are developed at each nodal point with the solution of these equations being the solution of the system. In the procedure, displacements of, and loads or stresses acting on the structure are replaced by equivalent values acting at the nodal points of the finite-element system. Since each element may have separate mechanical properties and loading, multimaterial or orthotropic motor case properties and structures of arbitrary geometry can be evaluated. The effects of finite length, curve boundaries, variable boundary conditions, and thermal expansion with temperatures are considered in the solution.

3. Propellant Properties and Allowables

Full characterization of the mechanical properties and bond and strain allowables of the qualification batch of ANB-3289-3 propellant was described earlier in this report. Properties of all materials used in the analysis are given in Figure 34. The modulus of elasticity of the propellant used in the analyses was obtained from Figure 14 using the time-temperature-shift-factor from Figure 15. The bond strength allowables are obtained by factoring the bond strength

(1) E. B. Becker and J. J. Brisbane, "Application of the Finite Element Method to Stress Analysis of Solid Propellant Rocket Grains", Report No. S-76, Vol. 1 and 2. Rohm and Haas Company, Redstone Arsenal Research Division, Huntsville, Alabama, January 1966.

MATERIALS PROPERTIES USED IN STRESS ANALYSIS

		Propellant ANB-3289-3	Liner SD-886	Insulation V-4030	Case Titanium
Modulus of Elasticity, N/cm^2 (psi)	Storage at 21°C for 3 Months	594 (860)	259 (360)	2,620 (3,800)	1105×10^4 (16×10^6)
	Firing at 21°C Time = 0.1 sec	(2,400)	(700)	(14,000)	
Poisson's Ratio, ν		0.5	0.5	0.5	0.29
Coefficient of Thermal Expansion, m/m/°C (in./in./°F)		11.0×10^{-5} (6.1×10^{-5})	11.3×10^{-5} (6.3×10^{-5})	18×10^{-5} (10×10^{-5})	8.3×10^{-6} (4.6×10^{-6})

Figure 34

averages from Figures 24, 19, or 21 for storage shear and firing shear, respectively. The factor is the bracketted quantity in the following equation:

$$\sigma_a = \bar{Y} \{1 - (3 + a) V_\sigma\}$$

Where σ_a = stress allowable

$\bar{Y}$ = average ultimate strength

a = statistical constant

V_σ = batch-to-batch coefficient of variation for stress

Using a = 1.645 for one batch and 95% confidence level and $V_\sigma = 0.1$ the factor becomes 54 percent.

The strain allowable for storage is obtained by factoring the strain from Figure 6. The factor is the bracketted quantity in the following equation:

$$\varepsilon_a = \bar{X} \left\{ \frac{1 - (3 + a) V_\varepsilon}{C_B} \right\}$$

Where ε_a = strain allowable

$\bar{X}$ = average ultimate failure strains

a = statistical constant

V_ε = batch-to-batch coefficient of variation for stress

C_B = correction for biaxiality

Using a = 1.645 for one batch and 95% confidence level, $V_\varepsilon = 0.1$ and $C_B = 1.2$ the factor becomes 45 percent. The strain allowable for firing is obtained directly from Figure 13.

4. Results

a. Reference Design

The reference grain design selected is the simple case-bonded configuration shown in Figure 35. The inner bore radius of 12.4 cm (4.90 in.) yields a nominal web thickness of 9.68 cm (3.81 in.) with the inside case radius of 22.40 cm (8.820 in.), 4030 rubber insulation thickness of 2.03 mm (0.080 in.) and SD-886 liner thickness of 0.76 mm (0.030 in.). The aft end of the grain is tapered to minimize the high stress peak characteristically encountered at the end of a bond. For this configuration under the condition of thermal shrinkage, the maximum tensile stress occurs at the forward end, and the maximum shear stress occurs at about 2.5 cm (1.0 in.) from the end of the bond.

b. Critical Loads

The loads imposed by thermal shrinkage were found to be much more severe than those resulting from motor firing. This was accentuated by the unexpectedly large shift in stress-free temperature measured under sterilization conditions. Instead of the differential temperature (ΔT) of 36°C (65°F) between the propellant cure temperature (initial stress-free temperature) of 57°C (155°F) and the nominal storage temperature of 21°C (70°F), the apparent stress-free temperature of 131°C (268°F) increases the ΔT (and therefore the shrinkage load) to 110°C (198°F), or by a factor of 3.0. Although the tests indicated the probability during motor sterilization of a lower stress-free temperature (due to tensile loading while cooling), it is prudent for design purposes to assume a full shift in stress-free temperature to the sterilization condition of 135°C (275°F), or a ΔT of 114°C (205°F).

c. Case-Bonded Analysis

Because the test program for the determination of stress-free temperatures was concurrent with this task, it was convenient to present the storage condition grain stresses and strains in terms of stress-free temperature.

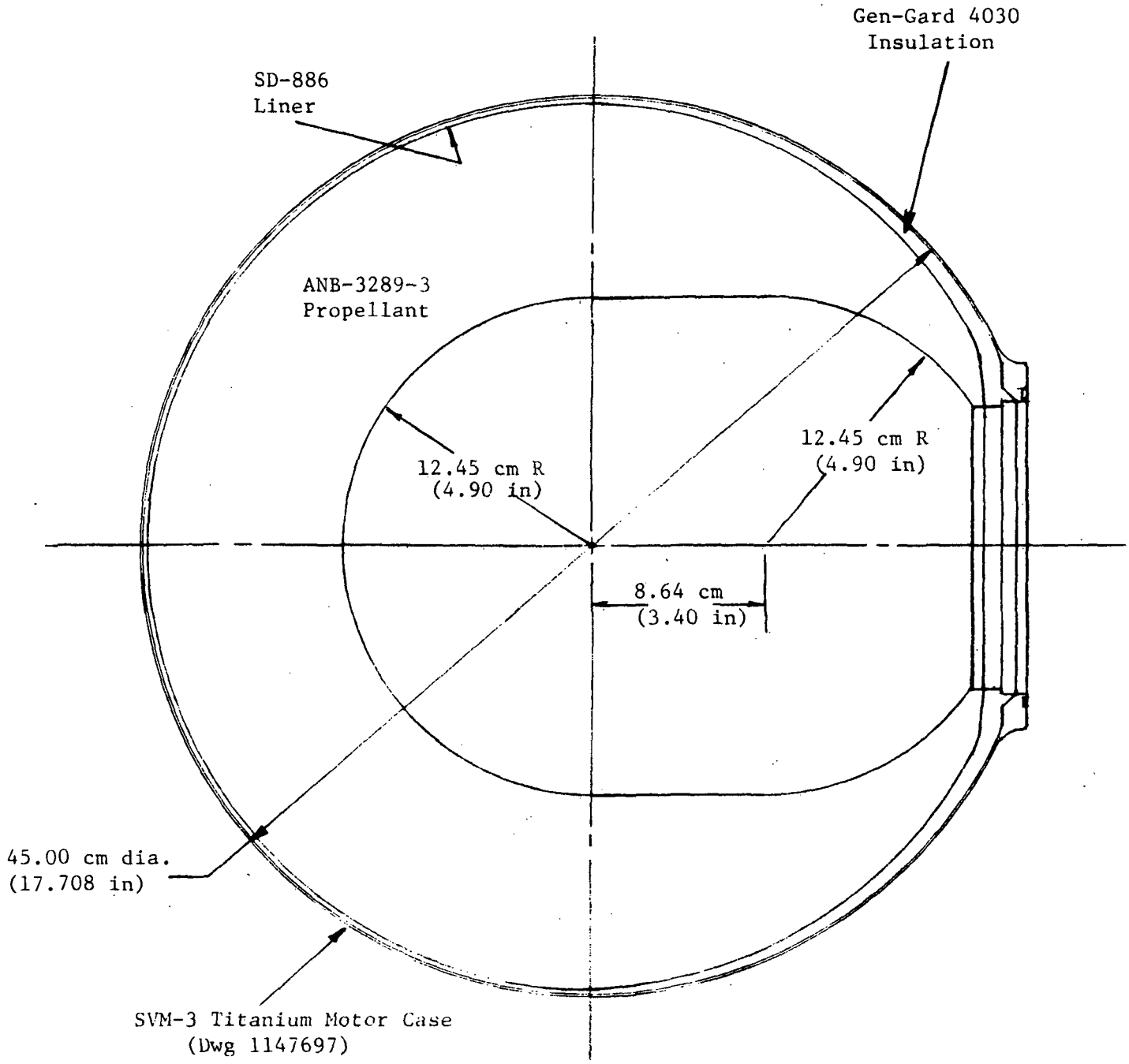

REFERENCE GRAIN DESIGN

Figure 35

Figure 36 gives the effect of stress-free temperature on maximum stresses and strains for the 21°C (70°F) storage condition. Zero margins of safety are encountered at stress-free temperatures of 58°C (137°F), 78°C (173°F) and 88°C (190°F) for tensile stress, shear stress and bore strain, respectively. This points out that, even with a conservative design and no stress-free temperature shift, the propellant allowables (relative to modulus) at long-term conditions are inferior to those usually encountered with typical composite propellants. The low strain allowable would be expected with this high-modulus propellant, but the propellant strength (and bond strength) are more typical of a low-modulus propellant. The reference design web thickness was reduced by 2.54 cm (1.00 in.) to produce more acceptable results, as shown also in Figure 36, but the zero margin on tensile stress can be seen to shift to only 86°C (187°F). Subsequently, tensile stress was calculated over a range of web thickness, as shown in Figure 37 for a series of stress-free temperatures. For a design condition stress-free temperature of 135°C (275°F) the web thickness must be reduced to only 5.08 cm (2.00 in.) to eliminate the negative margin. This would result in a motor volumetric loading of about 50%, which is a very inefficient design when compared to the loading of over 90% in the production SVM-3.

The fully bonded design presents no problems for firing. The maximum shear stress and bore strain are 53 N/cm^2 (77 psi) and 7.3 percent, respectively for the reference design assuming a stress-free temperature of 135°C (275°F). The allowable shear stress and strain for pressurization are (204 N/cm^2 (296 psi) and 17.5 percent, respectively.

d. Analysis of Released-Bond Concepts

The bulk of the analytical effort on the second design concept was expended on the sterilization cycling condition, as was done for the fully bonded grain or the first design concept. This effort was directed toward ways of reducing the bond restraint. Except for the bond pattern, they were identical to the reference grain design. Three bond patterns were investigated:

EFFECT OF STRESS-FREE TEMPERATURE ON MAXIMUM STRESSES AND STRAINS FOR CASE-BONDED GRAINS

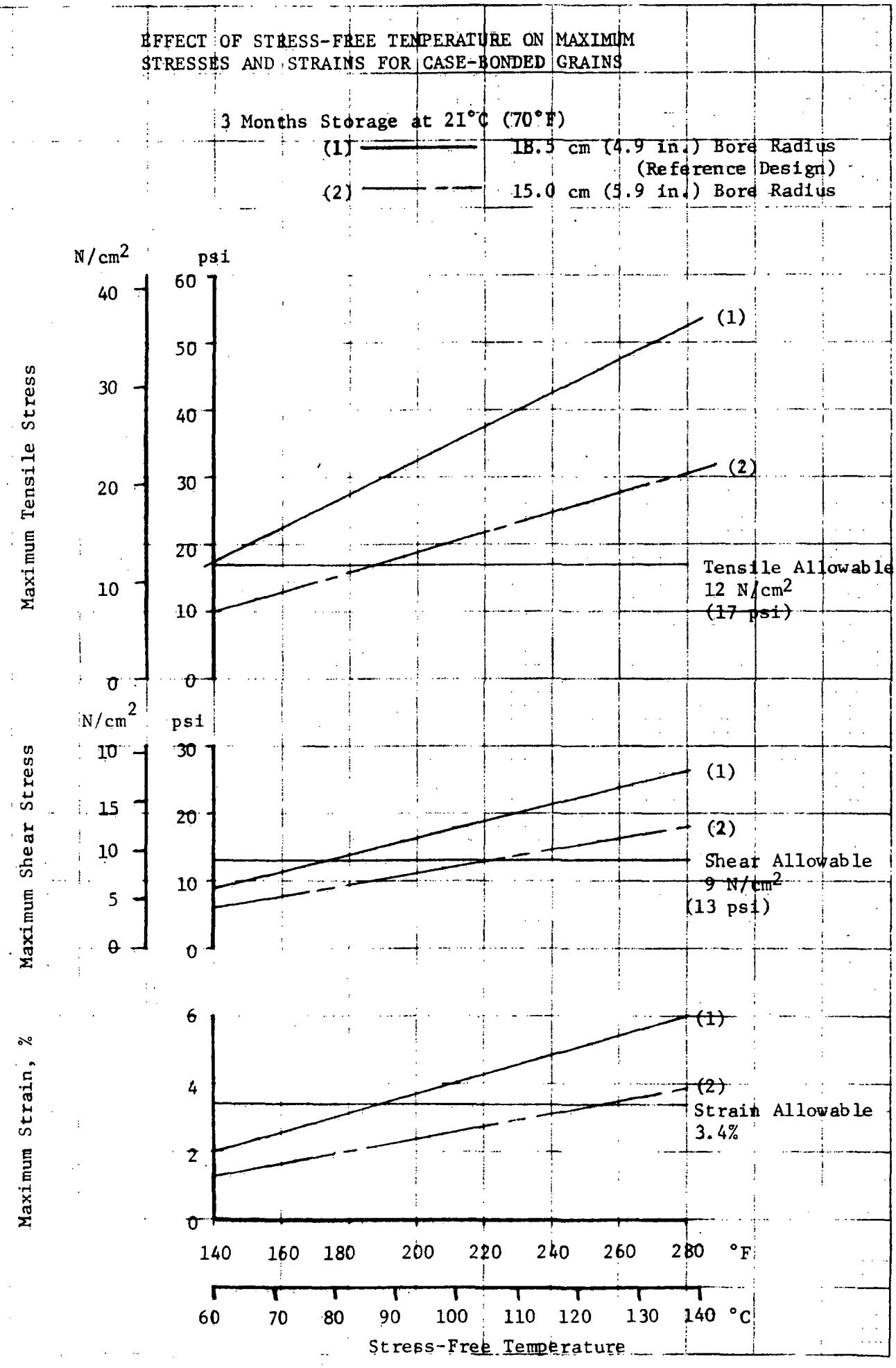

Figure 36

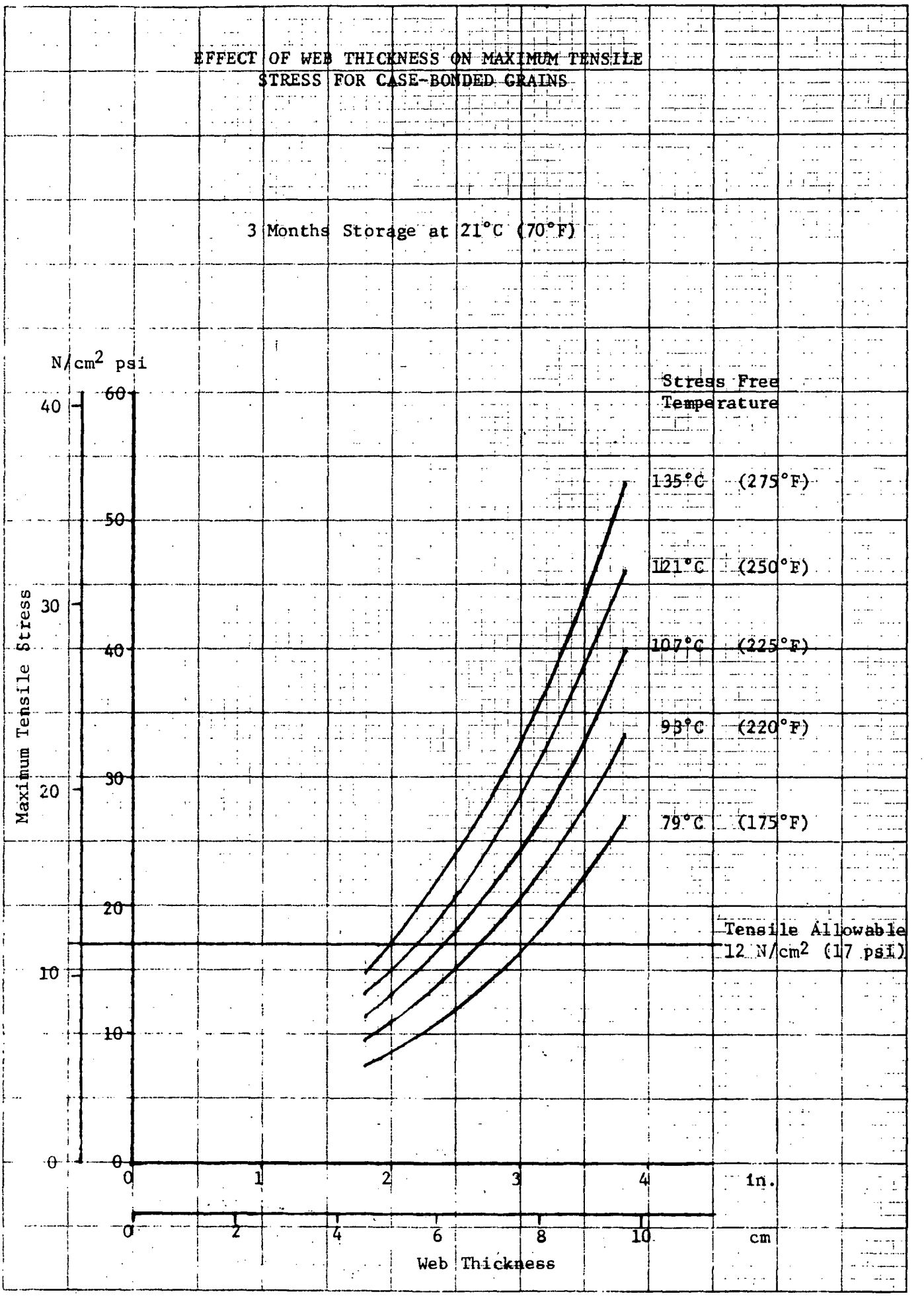
EFFECT OF WEB THICKNESS ON MAXIMUM TENSILE STRESS FOR CASE-BONDED GRAINS
3 Months Storage at 21°C (70°F)
N/cm² psi
Maximum Tensile Stress
Stress Free Temperature
135°C (275°F)
121°C (250°F)
107°C (225°F)
93°C (220°F)
79°C (175°F)
Tensile Allowable 12 N/cm² (17 psi)
0 1 2 3 4 in.
0 2 4 6 8 10 cm
Web Thickness

Figure 37

(1) Forward cap bond (45° half angle subtending the bonded cap).

(2) Circumferential strip bond 10° half angle subtending the bonded band around the equator.

(3) Three circular spots (15° half angle subtending the bonded caps) equally spaced around the equator.

The first and second patterns were analyzed using the axisymmetric computer solution. The maximum calculated tensile stress, shear stress and bore strain versus stress-free temperature in Figure 38. For comparison the corresponding values for the fully bonded design are also shown. It is interesting to note that while the bore strain was reduced by the bond releasing the bond tensile stresses actually increased. This is because of the stress concentration at the edge of the bond.

The third bond pattern is more difficult to analyze because it is not axisymmetric. Strictly speaking it should be analyzed using a three dimensional analysis which requires a great deal of computer time to perform. The following planar analyses were performed on a cross section through the equator of the motor.

(1) Plane stress fully bonded.
(2) Plane strain fully bonded.
(3) Plane stress bonded 15° released 45° on a 60° segment.
(4) Plane strain bonded 15° released 45° on a 60° segment.

The results of these analyses are shown in Figure 39 in the same manner as Figure 38.

The only analyses which show sufficient stress reduction are the plane stress ones and they are unrealistically optimistic.

At present a concept of tabs, possibly metal shim stock, bonded to the inside surface of the titanium case at one end on one side and to

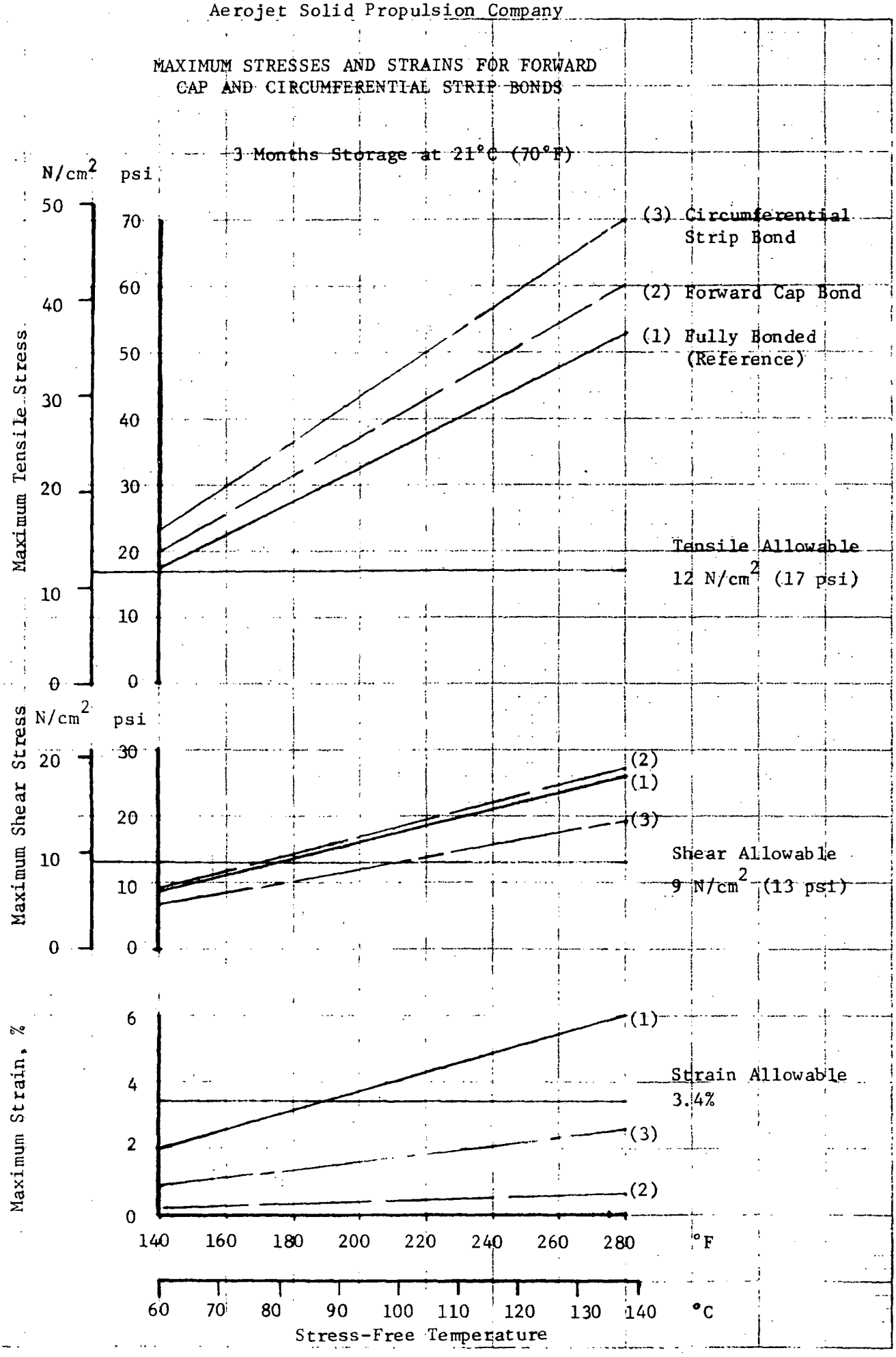
MAXIMUM STRESSES AND STRAINS FOR FORWARD CAP AND CIRCUMFERENTIAL STRIP BONDS
3 Months Storage at 21°C (70°F)
Maximum Tensile Stress
N/cm2
psi
(3) Circumferential Strip Bond
(2) Forward Cap Bond
(1) Fully Bonded (Reference)
Tensile Allowable
12 N/cm2 (17 psi)
Maximum Shear Stress
N/cm2
psi
Shear Allowable
9 N/cm2 (13 psi)
Maximum Strain, %
Strain Allowable
3.4%
°F
°C
Stress-Free Temperature

Figure 38

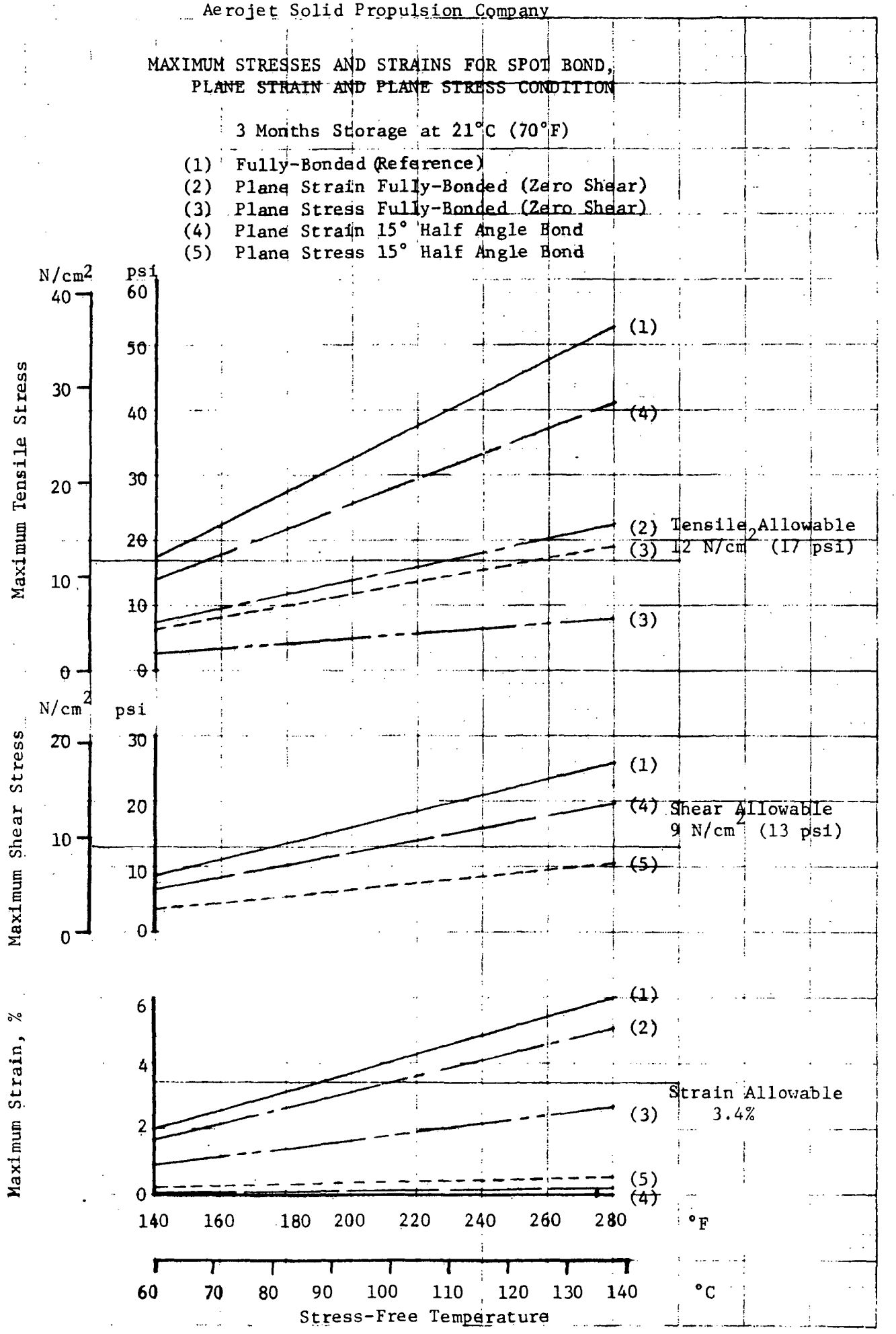
MAXIMUM STRESSES AND STRAINS FOR SPOT BOND,
PLANE STRAIN AND PLANE STRESS CONDITION
3 Months Storage at 21°C (70°F)
(1) Fully-Bonded (Reference)
(2) Plane Strain Fully-Bonded (Zero Shear)
(3) Plane Stress Fully-Bonded (Zero Shear)
(4) Plane Strain 15° Half Angle Bond
(5) Plane Stress 15° Half Angle Bond
N/cm2
psi
Maximum Tensile Stress
40
30
20
10
0
60
50
40
30
20
10
0
(1)
(4)
(2) Tensile Allowable
(3) 12 N/cm2 (17 psi)
(3)
N/cm2
psi
Maximum Shear Stress
20
10
0
30
20
10
0
(1)
(4) Shear Allowable
9 N/cm2 (13 psi)
(5)
Maximum Strain, %
6
4
2
0
(1)
(2)
Strain Allowable
3.4%
(3)
(5)
(4)
140 160 180 200 220 240 260 280 °F
60 70 80 90 100 110 120 130 140 °C
Stress-Free Temperature

Figure 39

to the outside surface of the insulation at the other end on the other side appears promising. Based on thermal concentration of 2.54 mm (0.1 in.) on the radius and 0.25 mm (0.01 in.) thick tabs 2.54 cm (1 in.) wide and cantilevered 2.54 cm (1 in.) from 6.45 cm^2 (1 $in.^2$) bond to 6.45 cm^2 1 $in.^2$) bond would produce tensile stress of approximately 0.69 N/cm^2 (1 psi). With 15 g's acceleration load the number of tabs required can be calculated assuming:

a. Tabs 50% (half in tension, half in compression) of 70% (approximate surface component of sphere) effective.

b. Allowable propellant-to-liner shear stress at time of 1 minute to be 34.5 N/cm^2 (50 psi), to be approximately 115 tabs. At a total area of tab of 19.35 cm^2 (3 $in.^2$) this would require tabs covering about 1/3 of the inside surface of the case.

Another concept worthy of investigation is similar to the one above but consisting of rubber disks. The middle of one side could be bonded to the inner surface of the chamber and the outer ring of the other side could be bonded to the insulation. This technique would allow a relative movement between the outside of the insulation and the inside of the case which would be very beneficial during sterilization cycling but at the same time maintain adequate grain retention to withstand acceleration loads.

CONCLUSIONS

A. PROPELLANT CHARACTERIZATION AND SCALE-UP

1. Modification of the sterilizable propellant formulation from 85 wt% to 84 wt% total solids did not show the gains in mechanical properties that had been anticipated.

2. As in the initial phase of this contract, the Telagen-S polymer lot produced in pilot plant quantities demonstrated propellant mechanical properties inferior to those previously demonstrated with the original laboratory-produced polymer.

3. Scale-up to a 75 kg (165 lb) size propellant batch had no apparent effect on propellant mechanical properties. Processing characteristics of the batch were more than adequate for full-scale motor casting requirements.

B. PROPELLANT STERILIZATION

Sterilization of the ANB-3289-3 formulation produced no physical defects. The standard tensile properties were unaffected by the six sterilization cycles, but the relaxation modulus was slightly affected.

C. STRESS-FREE TEMPERATURE DETERMINATION

Measurements of propellant specimens subjected to six sterilization cycles under compressive loads indicated large shifts in stress-free temperature to nearly the sterilization temperature. There is strong evidence of the load-path influence on the shifts, leading to the conclusion that stress-free temperature shifts may be effectively reduced by manipulation of the loading conditions. The behavior appears to be plastic in nature, indicating the dominance of changes in secondary bonds over chain cleavage and reformation.

D. GRAIN DESIGN ANALYSIS

1. The combination of low allowable strengths and the large sterilization-induced stress-free temperature shifts severely limits the efficient use of the sterilizable propellant for a case-bonded grain.

2. Various concepts of bond release patterns were ineffective in reducing bond tensile stress, which is the critical structural parameter for the spherical motor under storage conditions.

3. Unless the propellant characteristics can be greatly improved, some concept of a stress-relieving grain retention system will be necessary to allow the design of a practical grain with high volumetric loading.

RECOMMENDATIONS

A. It is recommended that additional work be directed toward propellant binder improvements. This would include both an upgrading of the polymer to improve propellant mechanical properties, and a re-evaluation of the secondary bond function at high temperatures to reduce stress-free temperature shifts.

B. It is recommended that further evaluation of stress-free temperature shifts explore the interaction of thermal environment and mechanical loads in the simulation of motor sterilization and cool-down in order to reduce the magnitude of stress-free temperature shifts.

C. It is recommended that stress relieving grain retention systems be evaluated for utilization of the existing-technology sterilizable propellant in a flight-weight motor.